Reliability-Based Geotechnical Engineering

Gordon A. Fenton[1] and D.V. Griffiths[2]

Keynote lecture presented at the ASCE GeoFlorida Conference
West Palm Beach, Florida, Feb 23, 2010

[1] Professor, Department of Engineering Mathematics, Dalhousie University, Halifax, Nova Scotia, Canada B3J 2X4; Ph: (902) 494-6002; email: Gordon.Fenton@dal.ca
[2] Professor, Division of Engineering, Colorado School of Mines, Golden, Colorado 80401-1887, USA; Ph: (303) 273-3669; email: D.V.Griffiths@mines.edu

ABSTRACT

The ground is a complex engineering material and how to characterize it realistically is a very difficult problem. It is well known that the engineering properties of the ground can vary quite dramatically from point to point throughout a site, and even more so from site to site, and that these properties are highly uncertain. It is also well known that the ground, when subjected to an imposed or self-load, will fail along its weakest path, however tortuous that might be.

Given the complexity of the ground, it makes sense to characterize the ground using models which allow for its quite uncertain spatial variability. It also makes sense to use response prediction models which take both spatial variability in ground properties and the tendency of failure to follow weakest paths through the ground into account.

The Random Finite Element Method (RFEM) combines spatially varying random field ground models with the finite element method to yield a reliability-based geotechnical methodology which accounts for both spatial variability and weakest path failure mechanisms. Besides being able to realistically model spatial variability in ground properties along with being able to follow the weakest path through the soil, mass, RFEM also provides the significant advantage of being able to account for site understanding in the design process.

This paper describes the Random Finite Element Method along with a few of its significant results over a variety of common geotechnical problems. The latter include ground-water modeling, shallow foundation settlement and bearing capacity, deep foundation capacity, and slope stability. LRFD code development will be discussed along the way.

INTRODUCTION

In an effort to harmonize with structural codes, geotechnical design codes around the world are beginning to migrate towards some form of reliability-based design (RBD). Significant steps in this direction can be found in, for example, Eurocode 7, 2003, Australian Standard AS 5100, 2004, AASHTO, 2007, and the National Building Code of Canada, 2005. These RBD provisions are most often presented in the form of a

Limit States Design (LSD), to define critical failure states, combined with load and resistance factors calibrated to achieve the target reliabilities associated with the various limit states. The use of load and resistance factors is generally referred to as Load and Resistance Factor Design (LRFD).

By and large, the random characteristics of loads, or "actions", in civil engineering projects, are fairly well known and so load factors are reasonably well established. On the resistance side, for most common structural materials representative tests can easily be performed, and have been, to establish material property distributions that apply with reasonable accuracy anywhere that the material is used. Thus, resistance factors for materials such as concrete, steel, and wood have been known for decades.

Unfortunately, the development of resistance factors for use in geotechnical engineering is much more difficult than for quality-controlled engineering materials, such as concrete, steel, or wood. For example, while the mean strength of a batch of 30 MPa concrete delivered to a site in one city, might differ by 5 to 10% from a batch delivered to a site in a second city, the soil strengths at the two sites may easily differ by orders of magnitude. A significant advantage of designing using quality-controlled materials is that the general form and, in particular, the variance of the material property distribution is well enough accepted by the engineering profession that only a few samples of the material are deemed necessary to ensure design requirements are met. That is, engineers rely on an *a priori* estimate of the material variance which means that testing can be aimed at only ensuring that the mean material resistance is sufficiently high (the number of samples taken is usually far too few to accurately estimate the variance). This is essentially a hypothesis test on the mean with variance known. Using this test to ensure that design requirements are met, combined with the known distributions and resulting codified load and resistance factors, is sufficient to provide a reasonably accurate reliability-based design.

Contrast the knowledge regarding the distribution of, say, concrete with that of soils. In analogy to the above discussion, it would be nice to have a reasonably accurate *a priori* estimate of soil property variance, so that only the mean soil property would have to be determined via a site investigation. This *a priori* variance for soils would generally be much larger than the actual variance at a single site, and its use would typically lead to significant overdesign in the attempt to achieve a certain reliability. In practice, due to the spatial persistence of ground properties, sites usually do not show the same level of variability that one sees over very large distances. In fact, it is the residual site specific variability about the locally estimated mean that governs site uncertainty. So the problem becomes how to determine a reasonable a priori site variance for use in reliability-base design?

The above discussion suggests that in order to achieve efficient reliability-based geotechnical designs, site investigations must be intensive enough to allow the estimation of both the soil mean and gain some idea of its variability – this level of site investigation intensity is typically what is aimed at in modern geotechnical codes, with varying degrees of success (for example, Australian Standard AS 4678, 2002, specifies three different investigation levels, associated with three different reliability levels). To date, however, little guidance is provided on how to determine "characteristic" design values for the soil on the basis of the gathered data, nor on how to use the estimated variance to adjust the design.

Another complicating factor, which is more of a concern in soils than in other quality-controlled materials, is that of spatial variability and its effect on design reliability. Soil properties often vary markedly from point to point and this variability can have quite different importance for different geotechnical issues. For example, footing settlement, which depends on an average property under the footing, is only moderately affected by spatial variability, while slope stability, which involves the path of least resistance, is more strongly affected by spatial variability. In this paper, spatial variability will be simply characterized by a parameter referred to here as the correlation length – small correlation lengths imply more rapidly varying properties, and so on. In order to adequately characterize the probabilistic nature of a soil and arrive at reasonable reliability-based designs, then, three parameters need to be estimated at each site; the mean, variance, and correlation length.

Fortunately, evidence compiled by the authors indicates that a 'worst case' correlation length typically exists – this means that, in the absence of sufficient data, this worst case can be used in reliability calculations. It will generally be true that insufficient data are collected at a site to reasonably estimate the correlation length, so the worst case value is conservative to use in design.

Once the random soil at a site has been characterized in some way, the question becomes how should this information be used in a reliability-based design? This paper describes the random finite element method along with some of its significant results for a number of common geotechnical problems. The tool can be used to assess geotechnical risk in design and to aid in the development of reliability-based geotechnical design codes.

All of the computer codes used in this paper are freely available at `http://www.engmath.dal.ca/rfem`. The website also contains a list of the papers by the authors which cover in considerably more detail the topics briefly presented here. The interested reader will also find a very comprehensive description of the background theory and all of these applications in Fenton and Griffiths (2008).

THE RANDOM FINITE ELEMENT METHOD

The Random Finite Element Method (RFEM) combines random field simulation and finite element (FE) analysis within a Monte Carlo framework. One of the great benefits of the finite element method is that it is easy to model problems with spatially variable properties. For example a given soil deposit may consist of layers having different permeability values in which rows of element may be assigned different properties. In the RFEM, this feature is taken to the limit by analyzing problems in which *every* element in the mesh has a different property based on some underlying statistical distribution. The finite element method used in RFEM is described in complete detail by Smith and Griffiths (2004).

Random fields are used to realistically represent the ground, allowing for the ground properties to varying spatially, as they do in nature. The simplest random field models follow a normal distribution. This is because the multi-variate normal distribution is relatively simple to use, both analytically and to simulate. A normal random field is characterized by a mean, μ, a variance, σ^2, and a correlation structure. The mean could be spatially varying, $\mu(x)$, and it is appropriate to do so when a trend has been identified at the site being modeled. In concept, the variance could also be

spatially varying, $\sigma^2(x)$, although this is rarely implemented since a very extensive site investigation would be required in order to even roughly estimate the variance trend. Generally, the variance is assumed to be *stationary*, in other words the same everywhere.

The most difficult aspect of random field models to both understand and estimate is its correlation structure. The purpose of a correlation structure is to provide for some 'persistence' in the random field – points close together will have similar properties while widely separated points could have quite different properties. This feature of random fields is what makes it a realistic soil model since, in general, real soils also tend to have similar properties at nearby points and less similar at larger separations.

Unfortunately, the correlation structure of a soil is very difficult to estimate even if a large data set is available. For this reason, correlation structures used in practice tend to be very simple, almost always requiring only a single parameter. One of the simplest and most widely used correlation structures is the Markov correlation function,

$$\rho(\tau) = \exp\left\{-\frac{2|\tau|}{\theta}\right\} \tag{1}$$

which gives the correlation coefficient between two points separated by distance τ. The single parameter, θ, is the *correlation length*, also called the *scale of fluctuation*. Roughly speaking, it is the separation distance beyond which two points in the field are largely uncorrelated (which, for a normal distribution, also means largely independent).

In practice, the estimation of the (directional) correlation length involves gathering data at a series of n equispaced locations along a line and fitting Eq. 1 to the sample correlation function,

$$\hat{\rho}(j\Delta x) = \frac{1}{(n-j-1)\hat{\sigma}_X^2}\sum_{i=1}^{n-j}(X_i - \hat{\mu}_X)\left(X_{i+j} - \hat{\mu}_X\right) \tag{2}$$

where Δx is the spacing between sample observations, $X_1, X_2, \ldots, X_n$, and $\hat{\mu}_X$ and $\hat{\sigma}_X$ are the estimated mean and standard deviations. Reasonably accurate estimates of $\hat{\rho}$ requires a large dataset, which for most geotechnical projects is not feasible. For almost all sites, the correlation length remains unknown, which is why the existence of a 'worst case' correlation length is so important. It allows a conservative reliability-based design to proceed without having to specifically know the correlation length. As will be shown in the following sections, the worst case correlation length tends to be of the same order of magnitude as characteristic dimensions of the problem under design (e.g. foundation width, distance to sampling location, etc.).

Once the theoretical nature of the random field has been decided upon (i.e. the distribution form and its mean, variance, and correlation structure) the next step in RFEM is the simulation of realizations of the random field. There are a variety of possible simulation algorithms available (see, e.g., Fenton, 1994) but the approach that the authors have elected to use in combination with the finite element method is the Local Average Subdivision (LAS) method (Fenton and Vanmarcke, 1990). The LAS method produces realizations of local averages of the random field, each local average taken over a region the same size as the finite elements they are then mapped to. There are a number of significant advantages to using local averages of ground properties in conjunction with finite element analysis;

1) finite elements are basically continuum representations of the material they model in which certain simplifying assumptions are made about the strain field within the element. For example, the shape functions of a 4-node quadrilateral element are exact if loading/displacements are applied at the nodes and the material properties within the element are constant. Thus, it is natural to assign the average of the random field over the element domain to that constant property.
2) the statistics of local averages (mean and variance) change as the size of the averaging domain changes, which is as specified by statistical theory. Thus, the use of a local average random field is also consistent with the finite element method in the sense that as the element (averaging domain) decreases, the representation of both the FE and LAS models tend harmoniously towards the point-wise varying random field.
3) most ground properties are measured as local averages in any case. For example, hydraulic conductivity is not measured at the atomic level – it is almost always a measure of the flow taking place through some volume of the permeable material, which is clearly an average of some sort. These physical measurements show the same variance reduction as the volume of the sample increases as do local averages of a random field. Thus, local averages are consistent with physical measurements of ground properties.

Figure 1 illustrates the basic idea behind Local Average Subdivision (see Fenton and Griffiths, 2008, for the details). The method proceeds iteratively by first randomly generating a local average for the entire field (Z_1^0) which has the correct statistics for an average of that dimension. The field is then subdivided into equal parts and the local averages Z_1^1 and Z_2^1 are generated in such a way that they have the correct average statistics, are properly correlated with one another, and average to the parent value, Z_1^0. The process is repeated, progressively subdividing the field until the desired resolution is achieved.

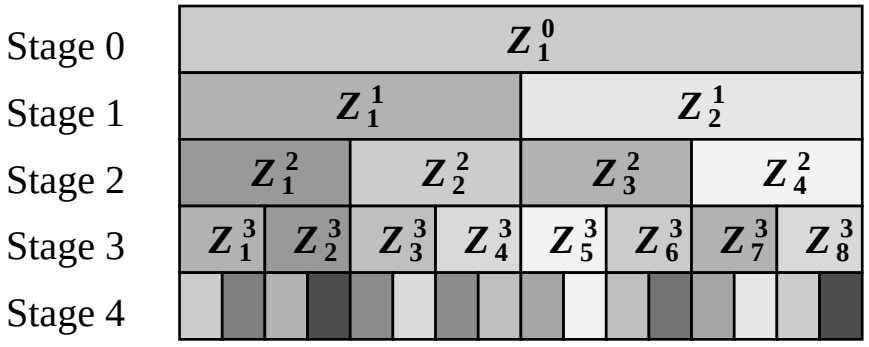

Figure 1. Top-down approach to LAS construction of a local average random process.

The final component of RFEM is the Monte Carlo simulation framework. Monte Carlo simulation is a very straightforward way to estimate means, variances, and probabilities associated with the response of complex systems to random inputs. While it is generally preferable to evaluate these response statistics and/or probabilities analytically, where

possible, we are often interested in systems which defy analytical solutions. For such systems, simulation techniques are ideal, since they are simple and lead to direct results. The main disadvantage of simulation derived moments or probabilities is that they do not lead to an understanding of how the probabilities or moments will change with changes in the system or input parameters. If the system is changed, the simulation must be repeated in order to determine the effect on response statistics and probabilities. In that analytical solutions are often not possible, this is usually an acceptable trade-off.

Monte Carlo simulation basically involves randomly generating a realization of the spatially variable ground properties, determining the response of the geotechnical system by a finite element analysis, and then repeating many times to estimate probabilities and statistics of the response. An important question that arises is, how many realizations should be performed in order to estimate probabilities, such as the probability of failure p_f, to within some acceptable accuracy? This question is reasonably easily answered by recognizing that each realization is a Bernoulli random variable that either fails or doesn't. The standard deviation of the probability estimate, $\hat{p}_f$ is then given by

$$\sigma_{\hat{p}_f} \simeq \sqrt{\frac{\hat{p}_f \hat{q}_f}{n}} \tag{3}$$

where the estimate of p_f is used (since p_f is unknown) and $\hat{q}_f = 1 - \hat{p}_f$.

In general, if the maximum acceptable error on p_f is e at confidence level $(1-\alpha)$, then the required number of realizations to achieve this accuracy is

$$n = \hat{p}_f \hat{q}_f \left(\frac{z_{\alpha/2}}{e}\right)^2 \tag{4}$$

where $z_{\alpha/2}$ is the point on the standard normal distribution having area (probability) $\alpha/2$ to the right.

We note that we are often interested in estimating very small failure probabilities – most civil engineering works have target failure probabilities between 1/1000 and 1/100,000. Estimating failure probabilities accurately in this range typically requires a very large number of realizations. Since the system response sometimes takes a long time to compute for each realization, for example when a non-linear finite element analysis is involved, large numbers of realizations may not be practical.

There are at least three possible solutions when a large number (e.g. hundreds of thousands or millions) of realizations are impractical;

1) perform as many realizations as practical, form a histogram of the response and fit a distribution to the histogram. The fitted distribution is then used to predict failure probabilities. The assumption here is that the distribution of the system response continues to be modeled by the fitted distribution in the tails of the distribution. This is often believed to be a reasonable assumption. In order to produce a reasonably accurate histogram, the number of realizations should still be relatively large (e.g. 500 or more).
2) develop an analytical model for the probability of failure by determining the distribution of the geotechnical response being studied. If the analytical model involves approximations, as they often do, some simulations should be performed to validate the model. The analytical model is then used to predict failure probabilities.

3) employ variance reduction techniques to reduce the required number of realizations to achieve a desired accuracy. In the context of random fields, these techniques tend to be difficult to implement and are not used by the authors. The interested reader is referred to Law and Kelton (2000) or Lewis and Orav (1989).

In summary, the Random Finite Element Method has a number of distinct advantages over most other common probabilistic methods;

1) The LAS method allows for the realistic, efficient, and statistically accurate modeling of soils, in which the representation of spatial variability is a natural component,
2) The FE method is a sophisticated analysis tool which allows the soil to fail along its weakest paths, without the need for *a priori* decisions about failure mechanisms and locations. As a result, the combination of LAS and FE methods is an important step forward in reducing geotechnical model error.
3) RFEM allows the effect of site investigation intensity on design reliability to be studied (see the Sections on Settlement and Bearing Capacity to follow). Because each random field realization is one possible 'picture' of the soil site, the entire investigation/design process is easily simulated. The effect of various sampling schemes on geotechnical system reliability is thus simply investigated. This ability, in turn, allows the method to provide quantitative probabilistic guidance in the development of reliability-based geotechnical design codes.

GROUND-WATER MODELING

Attention is now turned to the problem of steady-state seepage through a soil mass with spatially random permeability. The goal of this section is to present RFEM results which allow the assessment of probabilities relating to quantities of interest such as steady-state flow rates, exit gradients, and uplift pressures, although we will only present results relating to flow rates in this paper. The interested reader is directed to Griffiths and Fenton (1993) or Fenton and Griffiths (2008) for further details.

The equation of steady groundwater flow followed here is Laplace's equation

$$\nabla \cdot [\underset{\approx}{K} \nabla \phi] = 0 \tag{5}$$

where $\underset{\approx}{K}$ is the permeability tensor and ϕ is the hydraulic head.

To illustrate probabilistic ground-water modeling, a two-dimensional confined seepage problem is considered, with particular reference to flow under a water retaining structure founded on a stochastic soil. In the study of seepage through soils beneath water retaining structures, three important quantities need to be assessed by designers (see Figure 2); 1) seepage quantity, 2) exit gradients, and 3) uplift forces. The classical approach for estimating these quantities involves the use of carefully drawn flow nets (Casagrande 1937, Cedergren 1967, Verruijt 1970).

Various alternatives to flow nets are available for solving the seepage problem, however in order to perform quick parametric studies, for example relating to the effect of cut-off wall length, powerful approximate techniques such as the Method of Fragments (Pavlovsky 1933, Harr 1962, Griffiths 1984) are increasingly employed. The conventional methods are deterministic, in that the soil permeability is assumed to be *uniform* (everywhere the same), although anisotropic properties and stratification can be taken into account.

A more rational approach to the modeling of soil is to assume the permeability of the soil underlying a structure, such as that shown in Figure 2, is random, i.e. the soil is assumed to be a 'random' field (e.g. Vanmarcke 1984) characterized by a mean, standard deviation, and some correlation structure. While higher joint moments are possible, they are very rarely estimated with any accuracy, so generally just the first two moments (mean and covariance structure) are specified.

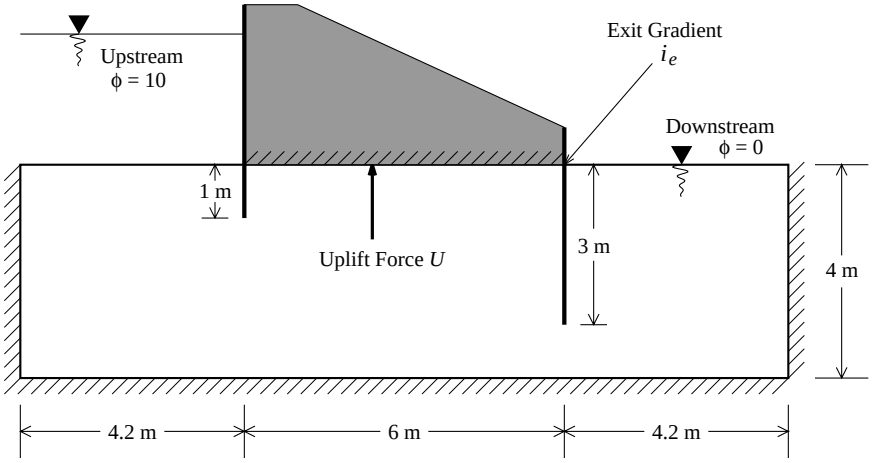

Figure 2. Confined seepage boundary value problem. The two vertical walls and the hashed boundaries are assumed impermeable.

The stochastic flow problem posed in Figure 2 is far too difficult to contemplate solving analytically (and/or the required simplifying assumption would make the solution useless). The determination of probabilities associated with flow, uplift, and exit gradients are conveniently done using RFEM, described above. In detail, the simulated field of permeabilities is mapped onto a finite element mesh, and potential and stream function boundary conditions are specified. The governing elliptic equation for steady flow (Laplace) leads to a system of linear 'equilibrium' equations which are solved for the nodal potential values throughout the mesh using conventional Gaussian elimination within a finite element framework.

Note that Eq. 5 is strictly only valid for spatially constant K. In this analysis the permeability is taken to be constant within each element, its value being given by the local geometric average of the permeability field over the element domain. The geometric average was found to be appropriate for square elements by Fenton and Griffiths (1993). From element to element, the value of K will vary, reflecting the random nature of the permeability.

Generation of Permeability Values

The permeability is assumed to be lognormally distributed and is obtained through the transformation

$$K_i = \exp\{\mu_{\ln K} + \sigma_{\ln K} G_i\} \tag{6}$$

in which K_i is the permeability assigned to the ith element, G_i is the local (arithmetic) average of a standard Gaussian random field, $G(\underset{\sim}{x})$, over the domain of the ith element,

and $\mu_{\ln K}$ and $\sigma_{\ln K}$ are the mean and standard deviation of the logarithm of K (obtained from the 'target' mean and standard deviation μ_K and σ_K).

Realizations of the permeability field are produced using LAS, discussed above, which renders realizations of local averages, G_i, of a random field $G(\underset{\sim}{x})$ having zero mean, unit variance, and a spatial correlation correlation length, $\theta_{\ln K}$. As the correlation length goes to infinity, G_i becomes equal to G_j for all elements i and j – that is the field of permeabilities tends to become uniform on each realization. At the other extreme, as the correlation length goes to zero, G_i and G_j become independent for all $i \neq j$ – the soil permeability changes rapidly from point to point.

In the two dimensional analyses presented in this section, the correlation lengths in the vertical and horizontal directions are taken to be equal (isotropic) for simplicity. Since actual soils are frequently layered, the correlation length horizontally is generally larger than it is vertically. However, the degree of layering is site specific and is left to the reader as a refinement. The results presented here are aimed at establishing the basic probabilistic behaviour of flow under water retaining structures. In addition, the two-dimensional model used herein implies that the out-of-plane correlation length is infinite – soil properties are constant in this direction – which is equivalent to specifying that the streamlines remain in the plane of the analysis. This is clearly a deficiency of the two-dimensional model, however most of the characteristics of the random flow are nevertheless captured by the two-dimensional model (Griffiths and Fenton, 1995).

Before discussing the results from multiple realizations, an example of what a flow net might look like for a single realization is given in Figures 3a and 3b for permeability statistics μ_K = 1 m/s, σ_K = 1 m/s and $\theta_{\ln K}$ = 1.0 m.

In Figure 3a, the flow net is superimposed on a 'grey-scale' which indicates the spatial distribution of the permeability values. Dark areas correspond to low permeability and light areas to high permeability. The streamlines clearly try to 'avoid' the low permeability zones, but this is not always possible as some realizations may generate a complete 'blockage' of low permeability material in certain parts of the flow regime. This type of 'blockage' is most likely to occur where the flow route is compressed, such as under a cut-off wall. An example where this happens is shown in Figure 3b. Flow in these (dark) low permeability zones is characterized by the streamlines moving further apart and the equipotentials moving closer together. Conversely, flow in the (light) high permeability zones is characterized by the equipotentials moving further apart and the streamlines moving closer together. In both of these figures the contrast between stochastic flow and the smooth flow lines that would occur through a deterministic and uniform field, is clear. In addition, the ability for the streamlines to avoid low permeability zones means that the average permeability seen by the flow is higher than if the flow was constrained to pass through the low permeability zones. This ability to circumnavigate the blockages is why the geometric average is a better model for two-dimensional flow than is the harmonic average.

Although *local* variations in the permeability have an obvious effect on the *local* paths taken by the water as it flows downstream, *globally* the stochastic and deterministic flow nets exhibit many similarities. The flow is predominantly in a downstream direction, with the fluid flowing down, under and around the cut-off walls. For this reason the statistics of the output quantities might be expected to be rather insensitive to the geometry of the problem (e.g. length of walls etc.), and qualitatively similar to the

properties of a 1-d flow problem, aside from an average effective permeability which is higher than in the 1-d case.

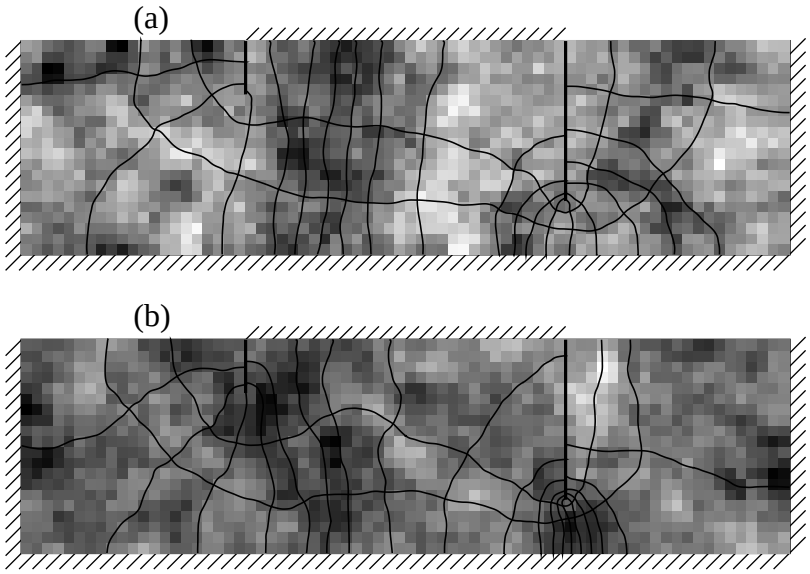

Figure 3. Stochastic flow net for two typical realizations.

Flow Rate Statistics

In the case of the flow rate, the global flow vector Q was computed by forming the product of the potentials and the global conductivity matrix $\tilde{K}$ in the finite element model. Assuming no sources or sinks in the flow regime, the only non-zero values in Q correspond to those freedoms on the upstream side at which the potentials were fixed equal to 10 m. These values were summed to give the total flow rate Q in $m^3/s/m$, leading to a non-dimensional flow rate $\bar{Q}$ defined by

$$\bar{Q} = \frac{Q}{\mu_K \Delta H} \tag{7}$$

where μ_k is the (isotropic) mean permeability and ΔH is the total head difference between the up- and downstream sides. $\bar{Q}$ is equivalent to the 'shape factor' of the problem, namely the ratio of the number of flow channels divided by the number of equipotential drops (n_f/n_d) that would be observed in a carefully drawn flow net; alternatively it is also equal to the reciprocal of the 'Form Factor' utilized by the Method of Fragments.

In the following, the distribution of $\bar{Q}$ will be investigated. The actual flow rate is determined by inverting Eq. 7,

$$Q = \mu_K \Delta H \bar{Q} \tag{8}$$

which will have the same distribution as $\bar{Q}$ except with mean and standard deviation,

$$\mu_Q = \mu_K \Delta H \mu_{\bar{Q}} \tag{9a}$$

$$\sigma_Q = \mu_K \Delta H \sigma_{\bar{Q}} \tag{9b}$$

Figure 4a shows a significant fall in $m_{\bar{Q}}$ (where $m_{\bar{Q}}$ is the simulation-based estimate of $\mu_{\bar{Q}}$) as σ_K/μ_K increases for $\theta_{\ln K} < 8$ m. As the correlation length approaches infinity, the expected value of $\bar{Q}$ approaches the constant 0.226. This curve is also shown in Figure 4a, although it should be noted it has been obtained through theory rather than simulation. In agreement with this result, the curve $\theta_{\ln K}$ = 8 m shows a less marked reduction in $m_{\bar{Q}}$ with increasing coefficient of variation σ_K/μ_K. However, over typical correlation lengths, the effect on average flow rate is slight. The decrease in flow rate as a function of the variability of the soil mass is an important observation from the point of view of design. Traditional design practice may very well be relying on this variability to reduce flow rates on average. It also implies that ensuring higher uniformity in the substrate may be unwarranted unless the mean permeability is known to be substantially reduced and/or the permeability throughout the site is carefully measured.

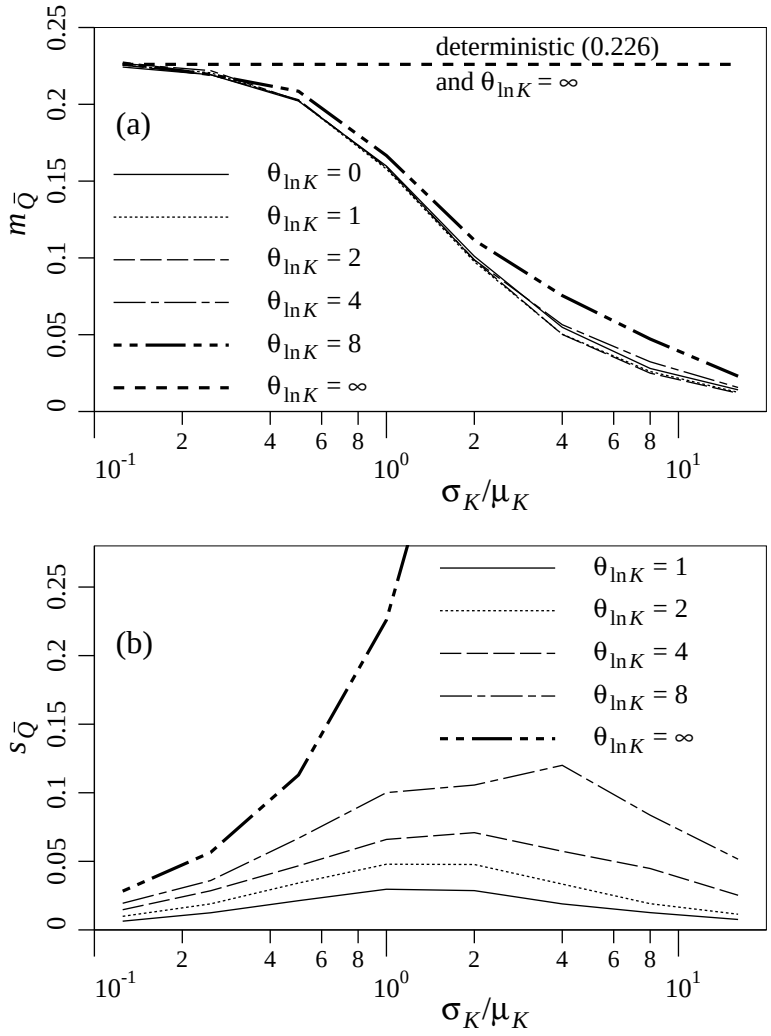

Figure 4. Effect of the correlation length and the coefficient of variation of permeability on a) the mean flow rate, and b) the flow rate standard deviation.

It may be noted that the deterministic result of $\bar{Q}$ = 0.226 has been included in Figure 4a, and as expected, the stochastic results converge on this value as σ_K/μ_K approaches zero.

Figure 4b shows the behaviour of $s_{\bar{Q}}$, the estimate of $\sigma_{\bar{Q}}$, as a function of σ_K/μ_K. Of particular note is that $s_{\bar{Q}}$ reaches a maximum corresponding to σ_K/μ_K in the range 1.0 - 2.0 for finite $\theta_{\ln K}$. Clearly, when σ_K = 0, the permeability field will be deterministic and there will be no variability in the flow rate: $\sigma_{\bar{Q}}$ will be zero. What is not quite so obvious is that because the mean of $\bar{Q}$ falls to zero when $\sigma_K/\mu_K \rightarrow \infty$ for finite $\theta_{\ln K}$ (see Figure 4 – the curves go to zero as the permeability variability increases), the standard deviation of $\bar{Q}$ must also fall to zero, since $\bar{Q}$ is nonnegative. Thus, $\sigma_{\bar{Q}}$ = 0 when the permeability variance is both zero and infinite. It must, therefore, reach a maximum somewhere between these two bounds. The point at which the maximum occurs moves to the right as $\theta_{\ln K}$ increases.

In general, it appears that the greatest variability in $\bar{Q}$ occurs under rather typical conditions: 'worst case' correlation lengths between 1 and 4 m and coefficient of variation of permeability of around 1 or 2.

SHALLOW FOUNDATION SETTLEMENT

Consider now a serviceability limit state, namely that of settlement of a shallow foundation. In structural design, serviceability limit states are investigated using unfactored loads and resistances. In keeping with this, both the Eurocode 7 (2003) and Australian Standard AS 2159 (1995) specify unit resistance factors for serviceability limit states. The Australian Standard AS 5100.3 (2004) states that "a geotechnical reduction factor need not be applied" for serviceability limit states.

Due to the inherently large variability of soils, however, and because settlement often governs a design, it is the opinion of the authors that properly selected resistance factors should be used for both ultimate and serviceability limit states in the settlement design of most geotechnical systems. The Australian Standard AS 4678 (2002), for example, agrees with this opinion and, in fact, distinguishes between resistance factors for ultimate limit states and serviceability limit states – the factors for the latter are closer to 1.0, reflecting the reduced reliability required for serviceability issues. Although the Canadian Foundation Engineering Manual (3rd Ed.,1992) suggests the use of a "performance factor" (foundation capacity reduction factor) of unity for settlement, it goes on to say "However, in view of the uncertainty and great variability in in situ soil-structure stiffnesses, Meyerhof (1982) has suggested that a performance factor of 0.7 should be used for an adequate reliability of serviceability estimates."

If resistance factors are to be used, how should they be selected so as to achieve a certain reliability? Statistical methods suggest that the resistance factors should be adjusted until a sufficiently small fraction of possible realizations of the soil enter the limit state being designed against. Unfortunately, there is only one realization of each site and, since all sites are different, it is difficult to apply statistical methods to this problem. For this reason geotechnical reliability-based code development has largely been accomplished by calibration with past experience as captured in previous codes. This is quite acceptable, since design methodologies have evolved over many years to produce a socially acceptable reliability, and this encapsulated information is very

valuable – see, for example, Vick's (2002) discussion of the value of judgement in engineering.

On the other hand, a reliability-based design code derived purely from deterministic codes cannot be expected to provide the additional economies that a true reliability-based design code could provide, eg. by allowing the specification of the target reliability (lower reliability for less important structures, etc.), or by improving the design as uncertainty is reduced, and so on. To attain this level of control in a reliability-based design code, probabilistic modeling and/or simulation of many possible soil regimes should also be employed to allow the investigation of the effect that certain design parameters have on system reliability. This is an important issue – it means that probabilistic modeling is necessary if reliability-based design codes are to evolve beyond being mirror images of the deterministic codes they derive from. The randomness of soils must be acknowledged and properly accounted for.

This section presents some results of a study in which a reliability-based settlement design approach is proposed and investigated via simulation using the Random Finite Element Method (RFEM). In particular, the effect of a soil's spatial variability and site investigation intensity on the resistance factors is quantified. The results of the study can and should be used to improve and generalize "calibrated" code provisions based purely on past experience. Further details of this study are given by Fenton et al. (2005) or Fenton and Griffiths (2008).

The settlement problem considered is that of a rigid rough square pad footing founded on the surface of a three-dimensional linearly elastic soil mass underlain by bedrock at depth H, as illustrated in Figure 5. The soil property of primary interest to settlement is elastic modulus, E, which is taken to be spatially random and may represent both the initial elastic and consolidation behaviour. Its distribution is assumed to be lognormal for two reasons: the first is that a geometric average tends to a lognormal distribution by the central limit theorem and the effective elastic modulus, as 'seen' by a footing, was found to be closely represented by a geometric average, and the second is that the lognormal distribution is strictly nonnegative which is physically reasonable for elastic modulus. The correlation structure is assumed to be Markovian (see Eq. 1). Poisson's ratio, having only a relatively minor influence on settlement, is assumed to be deterministic and is set equal to 0.3.

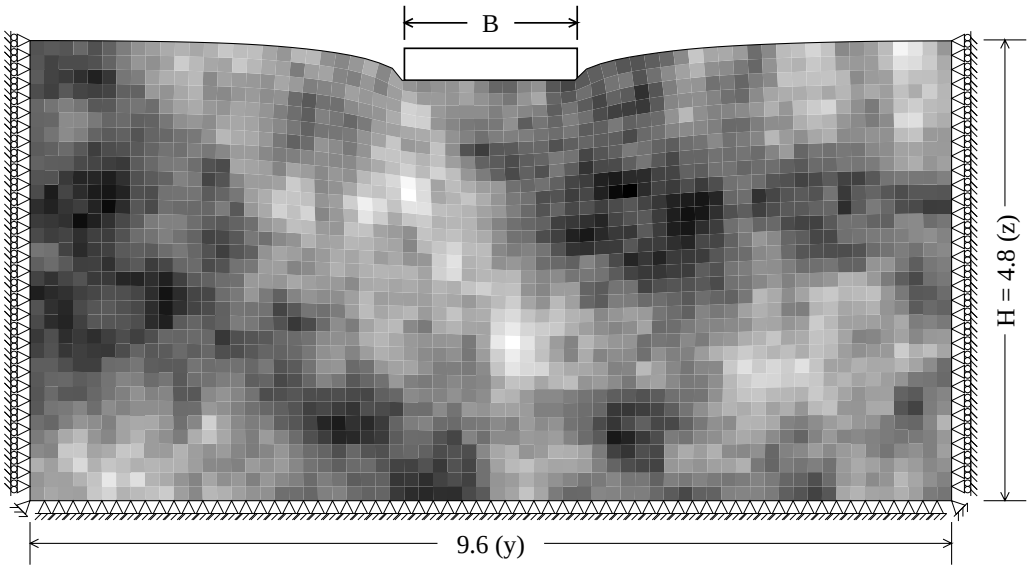

Figure 5. Cross-section through a realization of the random soil underlying the footing. Darker soils are stiffer.

Realizations of the random elastic modulus field are produced using the Local Average Subdivision (LAS) method which produces a discrete grid of local averages, G_i, of a standard Gaussian random field, having correlation structure given by Eq. 1, where averaging is performed over the domain of the i'th finite element. These local averages are then mapped to finite element properties according to

$$E_i = \exp\left\{\mu_{\ln E} + \sigma_{\ln E} G_i\right\} \tag{10}$$

Footing settlement is predicted here using a modified Janbu relationship (Janbu et al.,1956), and this is the basis of design used in this study;

$$\delta_p = u_1 \frac{\hat{q} B}{\hat{E}} \tag{11}$$

where δ_p is the predicted footing settlement, $\hat{q} = \hat{P}/B^2$ is the characteristic stress applied to the soil by the characteristic load, $\hat{P}$, acting over footing area $B \times B$, $\hat{E}$ is the estimate of elastic modulus underlying the footing, u_1 is an influence factor which includes the effect of Poisson's ratio (ν = 0.3 in this study). The characteristic load, $\hat{P}$, is often a nominal load computed from the supported live and dead loads, while the characteristic elastic modulus, $\hat{E}$, is usually a cautious estimate of the mean elastic modulus under the footing obtained by taking laboratory samples or by in-situ tests, such as CPT. In terms of the footing load, $\hat{P}$, the settlement predictor thus becomes

$$\delta_p = u_1 \frac{\hat{P}}{B\hat{E}} \tag{12}$$

The relationship above is somewhat modified from that given by Janbu et al. (1956) and Christian and Carrier (1978) in that the influence factor, u_1, is calibrated specifically for a square rough rigid footing founded on the surface of an elastic soil

using the same finite element model which is later used in the Monte Carlo simulations. This is done to remove bias (model) errors and concentrate specifically on the effect of spatial soil variability on required resistance factors. In practice, this means that the resistance factors suggested here are *upper bounds*, appropriate for use when bias and measurement errors are known to be minimal. A very close approximation to the finite element results is given by the fitted relationship

$$u_1 = 0.61 \left(1 - e^{-1.18H/B}\right) \tag{13}$$

Using Eq. 13 in Eq. 12 gives the following settlement prediction

$$\delta_p = 0.61 \left(1 - e^{-1.18H/B}\right) \left(\frac{\hat{P}}{B\hat{E}}\right) \tag{14}$$

The reliability-based design goal is to determine the footing width, B, such that the probability of exceeding a specified tolerable settlement, δ_{max}, is acceptably small. That is, to find B such that

$$\mathrm{P}\left[\delta > \delta_{max}\right] = p_f = p_m \tag{15}$$

where δ is the actual settlement of the footing 'as placed' (which will be considered here to be the same as 'as designed'). Design failure is assumed to have occurred if the actual footing settlement, δ, exceeds the maximum tolerable settlement, δ_{max}. The probability of design failure is p_f and p_m is the maximum acceptable probability of design failure.

A realization of the footing settlement, δ, is determined here using a finite element analysis of a realization of the random soil. For u_1 calibrated to the finite element results, δ can also be computed from

$$\delta = u_1 \frac{P}{BE_{eff}} \tag{16}$$

where P is the actual footing load and E_{eff} is the effective elastic modulus as seen by the footing (ie, the uniform value of elastic modulus which would produce a settlement identical to the actual footing settlement). Both P and E_{eff} are random variables.

One way of achieving the desired design reliability is to introduce a load factor, $\alpha \geq 1$, and a resistance factor, $\phi_g \leq 1$, and then finding B, α and ϕ_g which satisfy both Eq. 15 and Eq. 12 with $\delta = \delta_{max}$. In other words, find B and α/ϕ_g such that

$$\delta_{max} = u_1 \left(\frac{\alpha\hat{P}}{B\phi_g\hat{E}}\right) \tag{17}$$

and

$$\mathrm{P}\left[u_1 \frac{P}{BE_{eff}} > u_1 \left(\frac{\alpha\hat{P}}{B\phi_g\hat{E}}\right)\right] = p_m \tag{18}$$

In the above, we are assuming that the soil's elastic modulus, E, is the 'resistance' to the load and that it is to be factored due to its significant uncertainty.

Given α/ϕ_g, $\hat{P}$, $\hat{E}$, and H, Eq. 17 is relatively efficiently solved for B using a 1-pt iteration;

$$B_{i+1} = 0.61\left(1 - e^{-1.18H/B_i}\right)\left(\frac{\alpha\hat{P}}{\delta_{max}\phi_g\hat{E}}\right) \tag{19}$$

for $i = 0, 1, \ldots$ until successive estimates of B are sufficiently similar. A reasonable starting guess is $B_0 = 0.4(\alpha\hat{P})/(\delta_{max}\phi_g\hat{E})$.

Collecting all remaining random quantities leads to the simplified design probability

$$\mathrm{P}\left[P\frac{\hat{E}}{E_{eff}} > \frac{\alpha}{\phi_g}e^{\mu_{\ln P}}\right] = p_m \tag{20}$$

Simulation Results

The Random Finite Element Method (RFEM) will be employed within a design context to estimate settlement failure probabilities as a function of the resistance used in the design. The approach is described as follows;

1) decide on a maximum tolerable settlement, δ_{max}. To illustrate the approach we will select δ_{max} = 0.025 m.
2) estimate the characteristic footing load, $\hat{P}$, to be the median load applied to the footing by the supported structure (it is assumed that the load distribution is known well enough to know its median, $\hat{P} = e^{\mu_{\ln P}}$).
3) simulate an elastic modulus field, $E(\underset{\sim}{x})$, for the soil from a lognormal distribution with specified mean, μ_E, coefficient of variation, v_E, and correlation structure (e.g. Eq. 1) with correlation length $\theta_{\ln E}$.
4) 'virtually' sample the soil to obtain an estimate, $\hat{E}$, of its elastic modulus. In a real site investigation, the geotechnical engineer may estimate the soil's elastic modulus and depth to firm stratum by performing one or more CPT or SPT soundings. In this simulation, one or more vertical columns of the soil model are selected to yield the elastic modulus samples and $\hat{E}$ is set equal to their geometric average.
5) letting $\delta_p = \delta_{max}$, and for given factors α and ϕ_g solve Eq. 19 for B. This constitutes the footing design. Note that design widths are normally rounded up to the next most easily measured dimension (eg 1684 mm would probably be rounded up to 1700 mm). In the same way, in this analysis the design value of B is rounded up to the next larger element boundary, since the finite element model assumes footings are a whole number of elements wide. (The finite element model uses elements which are 0.15 m wide, so B is rounded up here to the next larger multiple of 0.15 m.)
6) simulate a lognormally distributed footing load, P, having median $\hat{P}$ and variance σ_P^2.
7) compute the 'actual' settlement, δ, of a footing of width B under load P on a random elastic modulus field using the finite element model. In this step, the virtually sampled random field generated in step (3) above is mapped to the finite element mesh, the footing of width B (suitably rounded up to a whole number of elements wide) is placed on the surface and the settlement computed by finite element analysis.

8) if $\delta > \delta_{max}$, the footing design is assumed to have failed.
9) repeat from step (3) a large number of times (n = 1000, in this study), counting the number of footings, n_f, which experienced a design failure. The failure probability is then estimated as $\hat{p}_f = n_f/n$.

By repeating the entire process over a range of possible values of ϕ_g the resistance factor which leads to an acceptable probability of failure, $p_f = p_m$, can be selected. This 'optimal' resistance factor will also depend on;

1) the number and locations of sampled columns (analogous to the number and locations of CPT/SPT soundings),
2) the coefficient of variation of the soil's elastic modulus, $v_{_E}$,
3) the correlation length, $\theta_{\ln E}$,

The simulation will be repeated over a range of values of these parameters to see how they affect ϕ_g.

Five different sampling schemes will be considered in this study, as illustrated in Figure 6 (see Jaksa et al., 2005, for a detailed study of the effectiveness of site investigations). The outer solid line denotes the edge of the soil model, and the interior dashed line the location of the footing. The small black squares show the plan locations where the site is virtually sampled. It is expected that the quality of the estimate of E_{eff} will improve for higher numbered sampling schemes. That is, the probability of design failure will decrease for higher numbered sampling schemes, everything else being held constant.

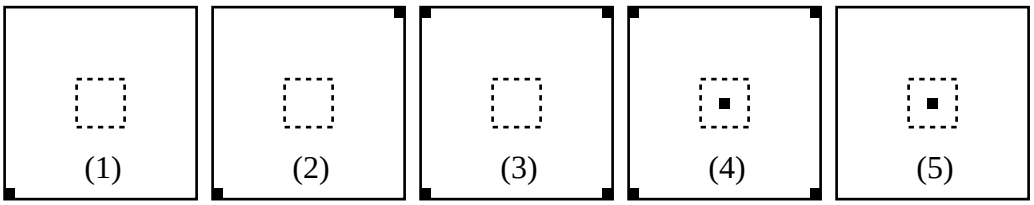

Figure 6. Sampling schemes considered in this study.

Figure 7 shows the effect of the correlation length on the probability of failure for sampling scheme #1 (a single sampled column at the corner of site) and for $v_{_E}$ = 0.5. The other sampling schemes and values of $v_{_E}$ displayed similarly shaped curves. Of particular note in Figure 7 is the fact that the probability of failure reaches a maximum for an intermediate correlation length, in this case when $\theta_{\ln E} \simeq$ 10 m. This is as expected, since for stationary random fields the values of $\hat{E}$ and E_{eff} will coincide for both vanishingly small correlation lengths (where local averaging results in both becoming equal to the median) and for very large correlation lengths (where $\hat{E}$ and E_{eff} become perfectly correlated) and so the largest differences between $\hat{E}$ and E_{eff} will occur at intermediate correlation lengths. The true maximum could lie somewhere between $\theta_{\ln E}$ = 1 m and $\theta_{\ln E}$ = 100 m in this particular study. This is a 'worst case' correlation length.

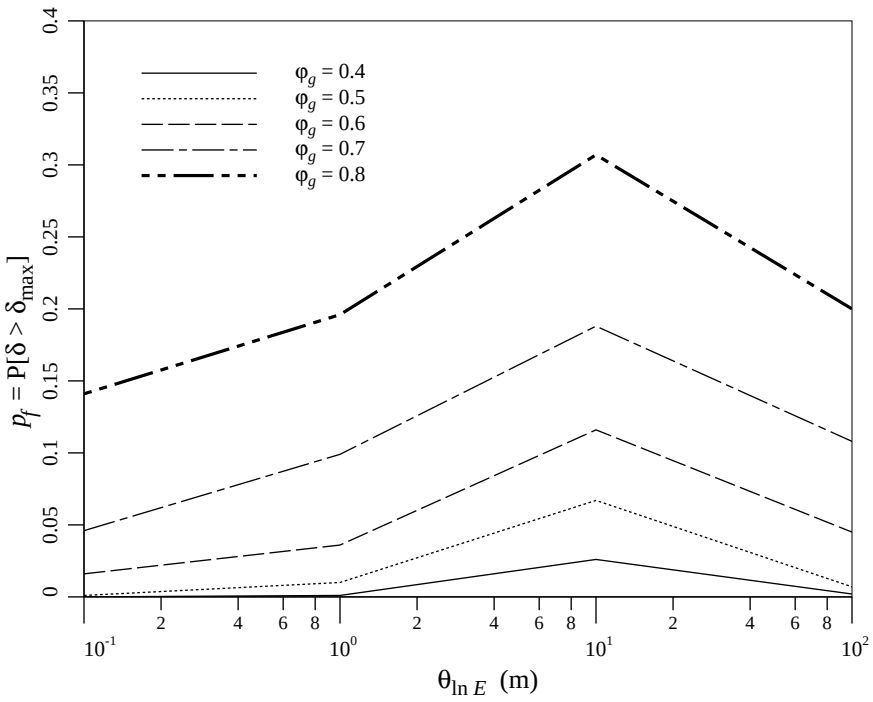

Figure 7. Effect of correlation length, $\theta_{\ln E}$, on probability of settlement failure, p_f = P [$\delta > \delta_{max}$].

Where the worst case correlation length occurs for arbitrary sampling patterns is still unknown. However, the authors expect that it is probably safe to say that taking $\theta_{\ln E}$ approximately equal to the average distance between sample locations and the footing center (but not less than the footing size) will yield suitably conservative failure probabilities. In the remainder of this study, the $\theta_{\ln E}$ = 10 m results will be concentrated on since these yielded the most conservative designs.

Figure 8 shows how the estimated probability of failure varies with resistance factor for the five sampling schemes considered with v_E = 0.5 and $\theta_{\ln E}$ = 10 m. This Figure can be used for design by drawing a horizontal line across at the target probability, p_m – to illustrate this, a light line has been drawn across at p_m = 0.05 – and then reading off the required resistance factor for a given sampling scheme. For example, if p_m = 0.05, then $\phi_g \simeq 0.46$ for the worst case sampling scheme #1.

As expected, improved sampling (i.e. improved site understanding) makes a significant difference to the required value of ϕ_g, which ranges from $\phi_g \simeq 0.46$ for sampling scheme #1 to $\phi_g \simeq 0.65$ for sampling scheme #5, assuming a target probability of p_m = 0.05. The implications of Figure 8 are that when soil variability is significant, considerable design/construction savings can be achieved when the sampling scheme and site understanding are improved.

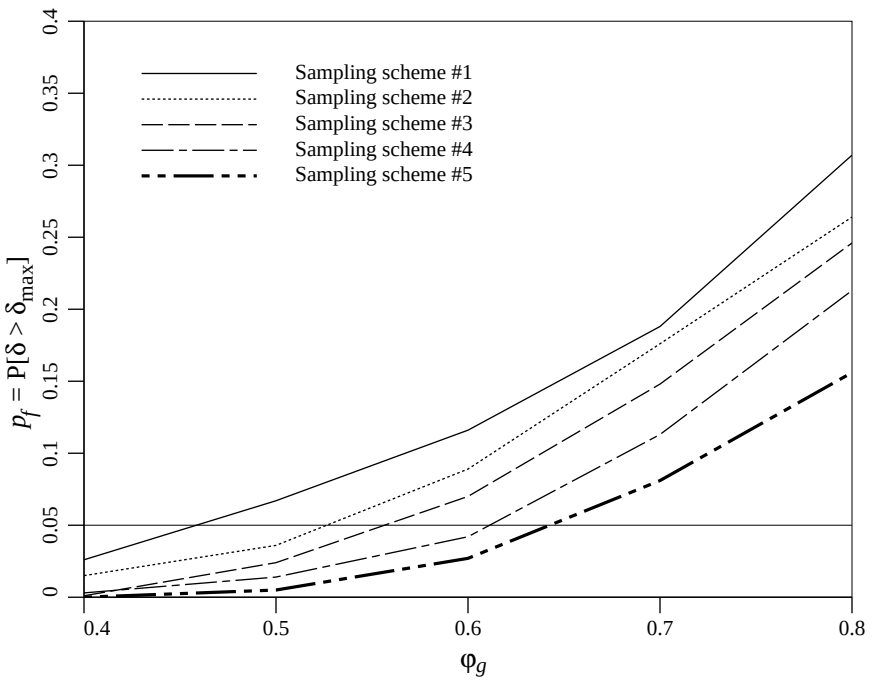

Figure 8. Effect of resistance factor, ϕ_g, on probability of failure, p_f = P [$\delta > \delta_{max}$] for v_E = 0.5 and $\theta_{\ln E}$ = 10 m.

SHALLOW FOUNDATION BEARING CAPACITY

The design of a shallow footing typically begins with a site investigation aimed at determining the strength of the founding soil or rock. Once this information has been gathered, the geotechnical engineer is in a position to determine the footing dimensions required to avoid entering various limit states. In so doing, it will be assumed here that the geotechnical engineer is in close communication with the structural engineer(s) and is aware of the loads that the footings are being designed to support. The limit states that are usually considered in the footing design are serviceability limit states (typically deformation – see previous section) and ultimate limit states. The latter is concerned with safety and includes the load-carrying capacity, or *bearing capacity*, of the footing.

This section investigates an LRFD approach for shallow foundations designed against bearing capacity failure. Only a few results are presented – the interested reader is directed to Fenton et al. (2008) or Fenton and Griffiths (2008) for more details.

The design goal is to determine the footing dimensions such that the *ultimate geotechnical resistance* based on characteristic soil properties, $\hat{R}_u$, satisfies

$$\phi_g \hat{R}_u \geq I \sum_i \alpha_i \hat{L}_i \tag{21}$$

where ϕ_g is the *geotechnical resistance factor*, I is an *importance factor*, α_i is the ith *load factor*, and $\hat{L}_i$ is the ith *characteristic load effect*. The relationship between ϕ_g and the probability that the designed footing will experience a bearing capacity failure will be summarized below (from Fenton et al., 2007) followed by some results on resistance factors required to achieve certain target maximum acceptable failure probabilities for the particular case of a strip footing (from Fenton et al., 2008). The symbol ϕ is commonly used to denoted the resistance factor – see, for example, the National Building Code of Canada (NBCC) [National Research Council (NRC), 2005] and in Commentary K "Foundations" of the User's Guide – NBC 2005 Structural Commentaries, NRC, 2006). The authors are also adopting the common notation where the subscript denotes the material that the resistance factor governs. For example, where ϕ_c and ϕ_s are resistance factors governing concrete and steel, the letter g in ϕ_g will be taken to denote "geotechnical" or "ground."

The importance factor in Eq. 21, I, reflects the severity of the failure consequences and may be larger than 1.0 for important structures, such as hospitals, whose failure consequences are severe and whose target probabilities of failure are much less than for typical structures. Typical structures usually are designed using I = 1, which will be assumed in this section. Structures with low failure consequences (minimal risk of loss of life, injury, and/or economic impact) may have $I < 1$.

Only one load combination will be considered in this section, $\alpha_L \hat{L}_L + \alpha_D \hat{L}_D$, where $\hat{L}_L$ is the characteristic live load, $\hat{L}_D$ is the characteristic dead load, and α_L and α_D are the live and dead load factors, respectively. The load factors will be as specified by the National Building Code of Canada (NBCC, 2006); α_L = 1.5 and α_D = 1.25. The theory presented here, however, is easily extended to other load combinations and factors, so long as their (possibly time-dependent) distributions are known.

The characteristic loads will be assumed to be defined in terms of the means of the load components in the following fashion,

$$\hat{L}_L = k_{L_e}\mu_{L_e} \tag{22a}$$

$$\hat{L}_D = k_D\mu_D \tag{22b}$$

where μ_{L_e} and μ_D are the means of the live and dead loads, respectively, and k_{L_e} and k_D are live and dead load *bias* factors, respectively. The bias factors provide some degree of 'comfort' by increasing the loads from the mean value to a value having a lesser chance of being exceeded. Since live loads are time varying, the value of μ_{L_e} is more specifically defined as the mean of the maximum live load experienced over a structure's lifetime (the subscript e denotes *extreme*).

For typical multistory office buildings, Allen (1975) estimates μ_{L_e} to be 1.7 kN/m^2, based on a 30 year lifetime. The corresponding characteristic live load given by the National Building Code of Canada (NBCC, 2006) is $\hat{L}_L$ = 2.4 kN/m^2, which implies that k_{L_e} = 2.4/1.7 = 1.41. Dead load, on the other hand, is largely static, and the time span considered (e.g. lifetime) has little effect on its distribution. Becker (1996) estimates k_D to be 1.18.

The characteristic ultimate geotechnical resistance $\hat{R}_u$ is determined using characteristic soil properties, in this case characteristic values of the soil's cohesion, c, and friction angle, ϕ (note that although the primes are omitted from these quantities it should be recognized that the theoretical developments described in this study are applicable to either total or effective strength parameters). To obtain the characteristic soil properties, the soil is assumed to be sampled over a single column somewhere in the vicinity of the footing, for example, a single CPT or SPT sounding near the footing. It is assumed here that the observations are error-free, which is an *unconservative* assumption. If the actual observations have considerable error, then the resistance factor used in the design should be reduced.

The characteristic value of the cohesion, $\hat{c}$, is defined here as the median of the sampled observations, c_i^o, which, assuming c is lognormally distributed, can be computed as a geometric average. The characteristic value of the friction angle is computed as an arithmetic average.

To determine the characteristic ultimate geotechnical resistance $\hat{R}_u$, it will first be assumed that the soil is weightless. This simplifies the calculation of the ultimate bearing stress q_u to

$$q_u = cN_c \tag{23}$$

The assumption of weightlessness is conservative since the soil weight contributes to the overall bearing capacity. This assumption also allows the analysis to explicitly concentrate on the role of cN_c on ultimate bearing capacity, since this is the only term that includes the effects of spatial variability relating to *both* shear strength parameters c and ϕ.

Bearing capacity predictions, involving specification of the N_c factor in this case, are generally based on plasticity theories (see, e.g., Prandtl, 1921; Terzaghi, 1943; and Sokolovski, 1965) in which a rigid base is punched into a softer material. These theories assume that the soil underlying the footing has properties which are spatially constant (everywhere the same). This type of ideal soil will be referred to as a *uniform*

soil henceforth. Under this assumption, most bearing capacity theories (e.g., Prandtl, 1921; Meyerhof, 1951, 1963) assume that the failure slip surface takes on a logarithmic spiral shape to give

$$N_c = \frac{e^{\pi \tan\phi} \tan^2\left(\frac{\pi}{4} + \frac{\phi}{2}\right) - 1}{\tan\phi} \tag{24}$$

The theory is derived for the general case of a $c - \phi$ soil. One can always set ϕ = 0 to obtain results for an undrained clayey soil.

Consistent with the theoretical results presented by Fenton et al. (2008), this section will concentrate on the design of a strip footing. In this case, the characteristic ultimate geotechnical resistance $\hat{R}_u$ becomes

$$\hat{R}_u = B\hat{q}_u \tag{25}$$

where B is the footing width and $\hat{R}_u$ has units of load per unit length out-of-plane, that is, in the direction of the strip foot. The characteristic ultimate bearing stress $\hat{q}_u$ is defined by

$$\hat{q}_u = \hat{c}\hat{N}_c \tag{26}$$

where the characteristic N_c factor is determined using the characteristic friction angle in Eq. 24.

For the strip footing and just the dead and live load combination, the LRFD equation becomes

$$\phi_g B\hat{q}_u = I\left[\alpha_L\hat{L}_L + \alpha_D\hat{L}_D\right] \quad \Longrightarrow \quad B = \frac{I\left[\alpha_L\hat{L}_L + \alpha_D\hat{L}_D\right]}{\phi_g\hat{q}_u} \tag{27}$$

To determine the resistance factor ϕ_g required to achieve a certain acceptable reliability of the constructed footing, it is necessary to estimate the probability of bearing capacity failure of a footing designed using Eq. 27. Once the probability of failure p_f for a certain design using a specific value for ϕ_g is known, this probability can be compared to the maximum acceptable failure probability p_m. If p_f exceeds p_m, then the resistance factor must be reduced and the footing redesigned. Similarly, if p_f is less than p_m, then the design is overconservative and the value of ϕ_g can be increased. A specific relationship between p_m and ϕ_g will be given below. Design curves will also be presented from which the value of ϕ_g required to achieve a maximum acceptable failure probability can be determined.

As suggested, the determination of the required resistance factor ϕ_g involves deciding on a maximum acceptable failure probability p_m. The choice of p_m derives from a consideration of acceptable risk and directly influences the size of ϕ_g. Different levels of p_m may be considered to reflect the "importance" of the supported structure – p_m may be much smaller for a hospital than for a storage warehouse. The choice of a maximum failure probability p_m should consider the margin of safety implicit in current foundation designs and the levels of reliability for geotechnical design as reported in the literature. The values of p_m for foundation designs are nearly the same or somewhat less than those for concrete and steel structures because of the difficulties and high expense of foundation repairs. Typical maximum acceptable failure probabilities of foundations range from 10^{-2} to 10^{-4} (Meyerhof, 1970). In general, these probabilities are deemed by the authors to be appropriate for designs involving low to high failure consequence

structures, with medium, or typical, failure consequence structures falling in the middle at about 10^{-3}.

We also note that the effect of structural importance is also typically reflected in the importance factor, I, of Eq. 21 and not in the resistance factor. The resistance factor should be aimed at a medium, or common, structural importance level and the importance factor should be varied above and below 1.0 to account for more and less important structures, respectively. However, since acceptable failure probabilities may not be simply connected to structural importance, we will assume $I = 1$ in the following. For code provisions, the factors recommended here should be considered to be the ratio ϕ_g/I

Random Soil Model

The soil cohesion c is assumed to be lognormally distributed with mean μ_c, standard deviation σ_c, and spatial correlation length $\theta_{\ln c}$. A lognormally distributed random field is obtained from a normally distributed random field $G_{\ln c}(\underset{\sim}{x})$ having zero mean, unit variance, and spatial correlation length $\theta_{\ln c}$ through the transformation

$$c(\underset{\sim}{x}) = \exp\{\mu_{\ln c} + \sigma_{\ln c} G_{\ln c}(\underset{\sim}{x})\} \tag{28}$$

where $\underset{\sim}{x}$ is the spatial position at which c is desired, $\sigma^2_{\ln c} = \ln\left(1 + v_c^2\right)$, $\mu_{\ln c} = \ln(\mu_c) - \sigma^2_{\ln c}/2$, and $v_c = \sigma_c/\mu_c$ is the coefficient of variation.

The correlation coefficient between the log-cohesion at a point $\underset{\sim}{x}_1$ and a second point $\underset{\sim}{x}_2$ is specified by a correlation function $\rho_{\ln c}(\underset{\sim}{\tau})$ where $\underset{\sim}{\tau} = \underset{\sim}{x}_1 - \underset{\sim}{x}_2$ is the vector between the two points. In this section, a simple exponentially decaying (Markovian) correlation function will be assumed (see Eq. 1).

The friction angle ϕ is assumed to be bounded both above and below, so that neither normal nor lognormal distributions are appropriate. A beta distribution is often used for bounded random variables. Unfortunately, a beta-distributed random field has a very complex joint distribution and simulation is cumbersome and numerically difficult. To keep things simple, a bounded distribution is selected which resembles a beta distribution but which arises as a simple transformation of a standard normal random field $G_\phi(\underset{\sim}{x})$ according to

$$\phi(\underset{\sim}{x}) = \phi_{min} + \tfrac{1}{2}(\phi_{max} - \phi_{min})\left\{1 + \tanh\left(\frac{sG_\phi(\underset{\sim}{x})}{2\pi}\right)\right\} \tag{29}$$

where ϕ_{min} and ϕ_{max} are the minimum and maximum friction angles in radians, respectively, and s is a scale factor which governs the friction angle variability between its two bounds. See Fenton and Griffiths (2008) more details about this distribution.

It seems reasonable to assume that if the spatial correlation structure of a soil is caused by changes in the constitutive nature of the soil over space, then both cohesion and friction angle would have similar correlation lengths. Thus, both cohesion and friction angle are assumed to have the same correlation structure. The two random fields, c and ϕ, are assumed to be independent which is deemed to be slightly conservative.

Nonzero correlations between c and ϕ were found by Fenton and Griffiths (2003) to have only a minor influence on the estimated probabilities of bearing capacity failure. Since the general consensus is that c and ϕ are negatively correlated (Cherubini, 2000;

Wolff, 1985) and the mean bearing capacity for independent c and ϕ was slightly lower than for the negatively correlated case (see Section 11.1), the assumption of independence between c and ϕ is slightly conservative.

Failure Probability

When soil properties are spatially variable, as they are in reality, then the hypothesis made in this study is that Eq. 23 can be replaced by

$$q_u = \bar{c}\bar{N}_c \tag{30}$$

where $\bar{c}$ and $\bar{N}_c$ are the *equivalent* cohesion and *equivalent* N_c factor, defined as those *uniform* soil parameters which lead to the same bearing capacity as observed in the real, spatially varying, soil. In other words, it is proposed that equivalent soil properties, $\bar{c}$ and $\bar{\phi}$, exist such that a uniform soil having these properties will have the same bearing capacity as the actual spatially variable soil. The value of $\bar{N}_c$ is obtained by using the equivalent friction angle $\bar{\phi}$ in Eq. 24.

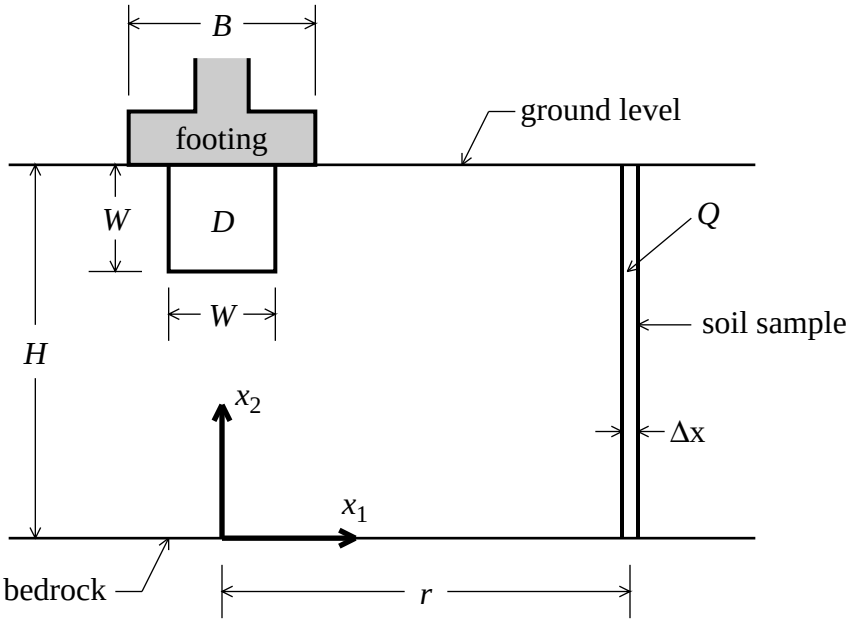

Figure 9. Averaging regions and distances used to predict probability of bearing capacity failure.

The design footing width B is obtained using Eq. 27, which, in terms of the characteristic design values, becomes

$$B = \frac{I\left[\alpha_L \hat{L}_L + \alpha_D \hat{L}_D\right]}{\phi_g \hat{c}\hat{N}_c} \tag{31}$$

The design philosophy proceeds as follows: Find the required footing width B such that the probability that the actual load L exceeds the actual resistance $q_u B$ is less than some small acceptable failure probability p_m. If p_f is the actual failure probability, then

$$p_f = \mathrm{P}\left[L > q_u B\right] = \mathrm{P}\left[L > \bar{c}\bar{N}_c B\right] \tag{32}$$

and a successful design methodology will have $p_f \leq p_m$. Substituting Eq. 31 into Eq. 32 and collecting random terms to the left of the inequality leads to

$$p_f = \mathrm{P}\left[L\frac{\hat{c}\hat{N}_c}{\bar{c}\bar{N}_c} > \frac{I\left[\alpha_L \hat{L}_L + \alpha_D \hat{L}_D\right]}{\phi_g} \right] \tag{33}$$

The footing shown in Figure 9 is just one possible realization since the footing width, B, is actually a random variable which depends on the results of the site investigation. In order to estimate failure probability analytically, the random c and ϕ fields are averaged over the domain D under the footing, where D is selected to approximately represent the volume of soil which deforms during a bearing capacity failure.

Figure 10 illustrates the best and worst agreement between failure probabilities estimated via simulation and those computed theoretically (Fenton et al., 2008). The failure probabilities are slightly underestimated at the worst-case correlation lengths when the sample location is not directly below the footing. Given all the approximations made in the theory, the agreement is very good (within a 10% relative error), allowing the resistance factors to be computed with confidence even at probability levels which the simulation cannot estimate – the simulation involved only 2000 realizations and so cannot properly resolve probabilities much less than 0.001.

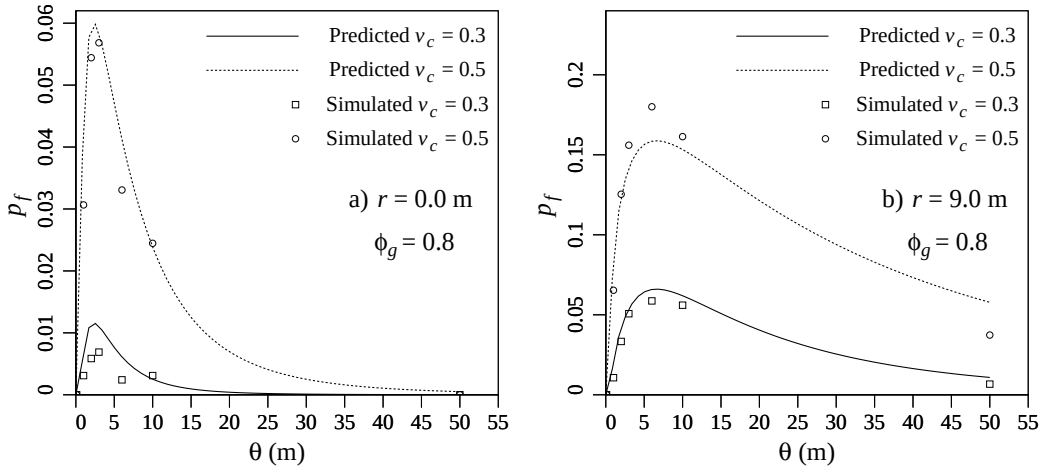

Figure 10. Comparison of simulation and theoretical (using Eq. 33) estimates of failure probabilities at two sampling distances.

Required Resistance Factor

Equation 33 can be inverted to find a relationship between the acceptable probability of failure $p_f = p_m$ and the resistance factor ϕ_g required to achieve an acceptable failure probability,

$$\phi_g = \frac{I\left[\alpha_L \hat{L}_L + \alpha_D \hat{L}_D\right]}{\exp\left\{\mu_{\ln Y} + \sigma_{\ln Y}\beta\right\}} \tag{34}$$

where $Y = L\hat{c}\hat{N}_c/(\bar{c}\bar{N}_c)$ and β is the desired reliability index corresponding to p_m.

Figure 11 shows the resistance factors required for the cases where the soil is sampled at a distance of 4.5 m from the footing centerline for a target maximum

acceptable failure probability of p_m = 10^{-3}. The worst-case correlation length is clearly between about 1 and 5 m, which is of the same magnitude as the mean footing width.

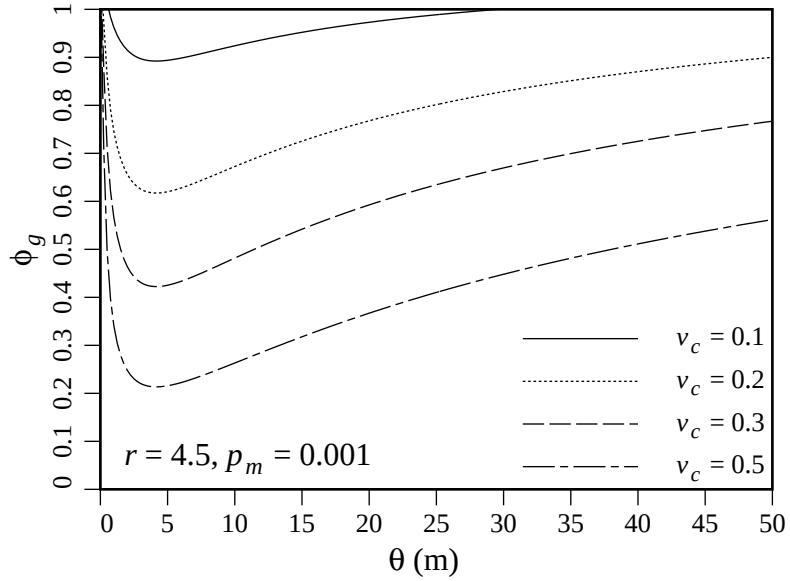

Figure 11. Resistance factors required to achieve acceptable failure probability p_m = 10^{-3} when soil is sampled at r = 4.5 m from footing centerline.

As expected the smallest resistance factors correspond to the worst case correlation lengths and the highest soil variability. In other words, there will be a significant construction cost penalty if a high reliability footing is designed using a site investigation which is insufficient to reduce the residual variability to less than v_c = 0.5.

One of the main impediments to the practical use of these results is that they depend on a-priori knowledge of the variance, and, to a lesser extent since worst-case results are presented above, the correlation structure of the soil properties. However, assuming that at least one CPT sounding (or equivalent) is taken in the vicinity of the footing, it is probably reasonable to assume that the residual variability is reduced to a coefficient of variation of no more than about 0.3, and often considerably less (the results collected by other investigators, e.g. Phoon et al., 1999, suggest that this may be the case for "typical" site investigations). If this is so, the resistance factors suggested for v_c = 0.3 are probably reasonable for the load and bias factors assumed in this study.

A significant advantage to formally relating the resistance factor to site understanding, such as shown in Figure 11, is that this provides geotechnical engineers with evidence that increased site investigation will lead to reduced construction costs and/or increased reliability. In other words, Figure 11 is further evidence that you pay for a site investigation whether you have one or not (Institution of Civil Engineers, 1991).

DEEP FOUNDATIONS

The resistance, or bearing capacity, of a pile arises as a combination of side friction, where load is transmitted to the soil through friction along the sides of the pile, and end bearing, where load is transmitted to the soil (or rock) through the tip of the pile. As load is applied to the pile, the pile settles – the total settlement of the pile is due to both deformation of the pile itself and deformation of the surrounding soil and supporting stratum. The surrounding soil is, at least initially, assumed to be perfectly bonded to the pile shaft through friction and/or adhesion so that any displacement of the pile corresponds to an equivalent local displacement of the soil (the soil deformation reduces further away from the pile). In turn, the elastic nature of the soil means that this displacement is resisted by a force which is proportional to the soil's elastic modulus and the magnitude of the displacement. Thus, at least initially, the support imparted by the soil to the pile depends on the elastic properties of the surrounding soil. For example, Vesic (1977) states that the fraction of pile settlement due to deformation of the soil, δ_s, is a constant (dependent on Poisson's ratio and pile geometry) times Q/E_s, where Q is the applied load and E_s is the (effective) soil elastic modulus.

As the load on the pile is increased, the bond between the soil and the pile surface will at some point break down and the pile will both slip through the surrounding soil and plastically fail the soil under the pile tip. At this point, the ultimate bearing capacity of the pile has been reached. The force required to reach the point at which the pile slips through a sandy soil is conveniently captured using a soil-pile interface friction angle, δ. The frictional resistance per unit area of the pile surface, f, can then be expressed as

$$f = \sigma'_n \tan\delta \tag{35}$$

where σ'_n is the effective stress exerted by the soil normal to the pile surface. In many cases, $\sigma'_n = K\sigma'_o$, where K is the earth pressure coefficient and σ'_o is the effective vertical stress at the depth under consideration. The total ultimate resistance supplied by the soil to an applied pile load is the sum of the end bearing capacity (which can be estimated using the usual bearing capacity equation) and the integral of f over the embedded surface of the pile. For clays with zero friction angle, Vijayvergiya and Focht (1972) suggest that the average of f, denoted with an overbar, can be expressed in the form

$$\overline{f} = \lambda\left(\overline{\sigma}'_o + 2c_u\right) \tag{36}$$

where $\overline{\sigma}'_o$ is the average effective vertical stress over the entire embedment length, c_u is the undrained cohesion, and λ is a correction factor dependent on pile embedment length.

The limit state design of a pile involves checking the design at both the serviceability limit state (SLS) and the ultimate limit state (ULS). The serviceability limit state is a limitation on pile settlement, which in effect involves computing the load beyond which settlements become intolerable. Pile settlement involves consideration of the elastic behaviour of the pile and the elastic (e.g. E_s) and consolidation behaviour of the surrounding soil.

The ultimate limit state involves computing the ultimate load that the pile can carry just prior to failure. Failure is assumed to occur when the pile slips through the soil (we are not considering structural failure of the pile itself) which can be estimated

with the aid of Eq's 35 or 36, along with the end bearing capacity equation. The ultimate pile capacity is a function of the soil's cohesion and friction angle parameters.

In this section, the soil's influence on the pile will be represented by bi-linear springs (see, e.g., Program 12 of Smith and Griffiths, 1982), as illustrated in Figure 12. The initial sloped portion of the load-displacement curve corresponds to the elastic (E_s) soil behaviour, while the plateau corresponds to the ultimate shear strength of the pile-soil interface which is a function of the soil's friction angle and cohesion. The next section discusses the finite element and random field models used to represent the pile and supporting soil in more detail. In the following section an analysis of the random behaviour of a pile is described and presented. Only the effects of the spatial variability of the soil are investigated, and not, for instance, those due to construction and placement variability. Finally, the results are evaluated and recommendations are made.

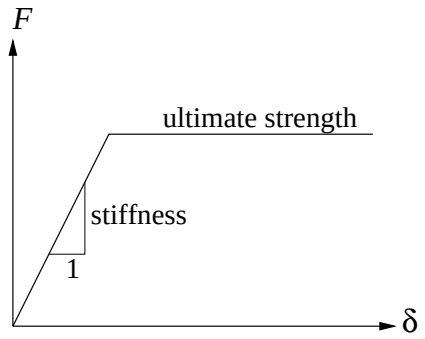

Figure 12. Bi-linear load (F) vs. displacement (δ) curve for soil springs.

The Random Finite Element Model

The pile itself is divided into a series of elements, as illustrated in Figure 13. Each element has cross-sectional area, A, (assumed constant) and elastic modulus, E_p, which can vary randomly along the pile. The stiffness assigned to the i^{th} element is the geometric average of the product AE_p over the element domain.

As indicated in Figure 12, the i^{th} soil spring is characterized by two parameters; its initial stiffness, S_i, and its ultimate strength, U_i. The determination of these two parameters from the soil's elastic modulus, friction angle, and cohesion properties is discussed conceptually as follows;

1) The initial spring stiffness, S_i, is a function of the soil's spatially variable elastic modulus, E_s. Since the strain induced in the surrounding soil due to displacement of the pile is complex, not least because the strain decreases non-linearly with distance from the pile, the effective elastic modulus of the soil as seen by the pile at any point along the pile is currently unknown. The nature of the relationship between E_s and S_i remains a topic for further research. In this chapter, the spring stiffness contribution per unit length of the pile, $S(z)$, will be simulated directly as a lognormally distributed one-dimensional random process.
2) The ultimate strength of each spring is somewhat more easily specified, so long as the pile-soil interface adhesion, friction angle, and normal stress are known. Assuming that soil properties vary only with depth, z, the ultimate strength per unit

pile length at depth z, will have the general form (in the event that both adhesion and friction act simultaneously)

$$U(z) = p\left[\alpha c_u(z) + \sigma'_n(z)\tan\delta(z)\right] \tag{37}$$

where $\alpha c_u(z)$ is the adhesion at depth z (see, e.g., Das, 2000, pg. 519, for estimates of the adhesion factor, α), p is the pile perimeter length, $\sigma'_n(z)$ is the normal effective soil stress at depth z, and $\delta(z)$ is the interface friction angle at depth z. The normal stress is often taken as $K\sigma'_o$, where K is an earth pressure coefficient. Rather than simulate c_u and $\tan\delta$ and introduce the empirical and uncertain factors α and K, both of which could also be spatially variable, the ultimate strength per unit length, $U(z)$, will be simulated directly as a lognormally distributed one-dimensional random process.

The random finite element model (RFEM) thus consists of a sequence of pile elements joined by nodes, a sequence of spring elements attached to the nodes (see Figure 13), and three *independent* 1-D random processes described as follows;

- $S(z)$ and $U(z)$ are the spring stiffness and strength contributions from the soil per unit length along the pile, and
- $E_p(z)$ is the elastic modulus of the pile.

It is assumed that the elastic modulus of the pile is a 1-D stationary lognormally distributed random process characterized by the mean pile stiffness, μ_{AE_p}, standard deviation, σ_{AE_p}, and correlation length $\theta_{\ln E_p}$, where A is the pile cross-sectional area. Note that for simplicity, it is assumed that all three random processes have the same correlation lengths and all have the same correlation function (Markovian). While it may make sense for the correlation lengths associated with $S(z)$ and $U(z)$ to be similar, there is no reason that the correlation length of $E_p(z)$ should be the same as that in the soil. Keeping them the same merely simplifies the study, while still allowing the study to assess whether a "worst case" correlation length exists for the deep foundation problem.

To assess the probabilistic behaviour of deep foundations, a series of Monte Carlo simulations, with 2000 realizations each, were performed and the distribution of the serviceability limit state loads were estimated. The serviceability limit state was defined as being a settlement of δ_{max} = 25 mm. Because the maximum tolerable settlement cannot easily be expressed in dimensionless form, the entire analysis will be performed for a particular case study; namely a pile of length 10 m is divided into n = 30 elements with μ_{AE_p} = 1000 kN, σ_{AE_p} = 100 kN, μ_S = 100 kN/m/m, and μ_U = 10 kN/m. The base of the pile is assumed to rest on a slightly firmer stratum, so the base spring has mean stiffness 200 kN/m and mean strength 20 kN (note that this is in addition to the soil contribution arising from the lowermost half-element). Coefficients of variation of spring stiffness and strength, v_S and v_U, taken to be equal and collectively referred to as v, ranged from 0.1 to 0.5. Correlation lengths, $\theta_{\ln S}$, $\theta_{\ln E_p}$, and $\theta_{\ln U}$, all taken to be equal and referred to collectively simply as θ, ranged from 0.1 m to 100.0 m. The spring stiffness and strength parameters were assumed to be mutually independent, as well as being independent of the pile elastic modulus.

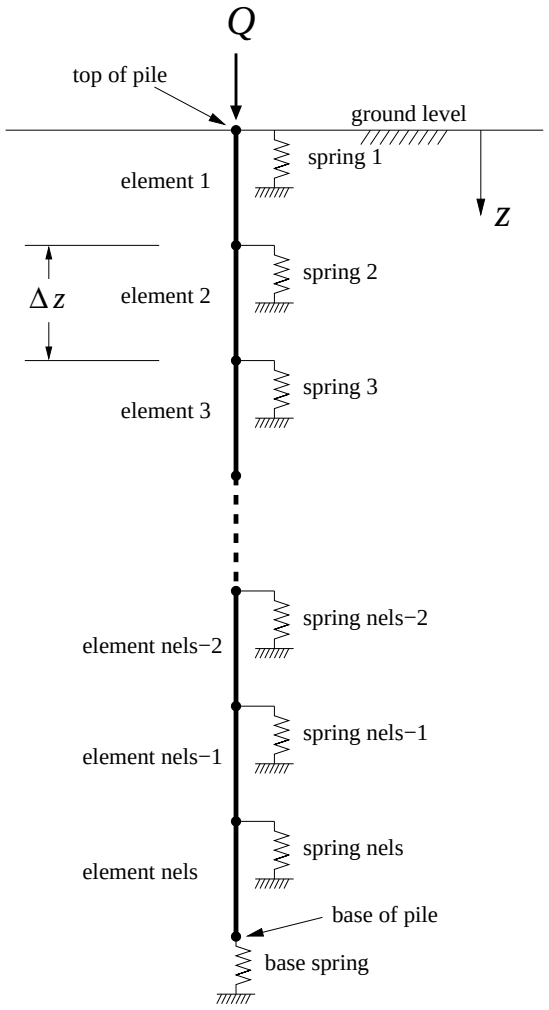

Figure 13. Finite element representation of the pile-soil system.

Figure 14 shows one of the best (on the left) and worst (on the right) fits of a lognormal distribution to the serviceability pile load histogram with chi-square goodness-of-fit p-values of 0.84 and 0.0006, respectively (the null hypothesis being that the serviceability load follows a lognormal distribution). The right-hand plot would result in the lognormal hypothesis being rejected for any significance level in excess of 0.06%. Nevertheless, a visual inspection of the plot suggests that the lognormal distribution is quite *reasonable* – in fact it is hard to see why one fit is so much 'better' than the other. It is well known, however, that when the number of simulations is large, goodness-of-fit tests tend to be very sensitive to small discrepancies in the fit, particularly in the tails.

In the case of the ultimate limit state, the pile capacity problem becomes much simpler – the ultimate capacity is just the sum of the ultimate spring strengths along the pile. What this means in practice is that the ultimate pile capacity is just the sum of ultimate shear forces provided by the supporting soil to the pile perimeter. In the case of an undrained soil, the ultimate resistance of a pile of length H (ignoring end-bearing) due to cohesion, c, between the pile surface and and its surrounding soil can be computed according to,

$$R_u = \int_0^H p\alpha c(z)\, dz \tag{38}$$

where p is the effective perimeter length of the pile section, $c(z)$ is the soil cohesion at depth z (locally averaged around the pile perimeter), and α is the ratio of the ultimate cohesion acting on the pile surface and the soil cohesion, which is typically somewhere between 0.5 and 1.0 (CFEM, 2006).

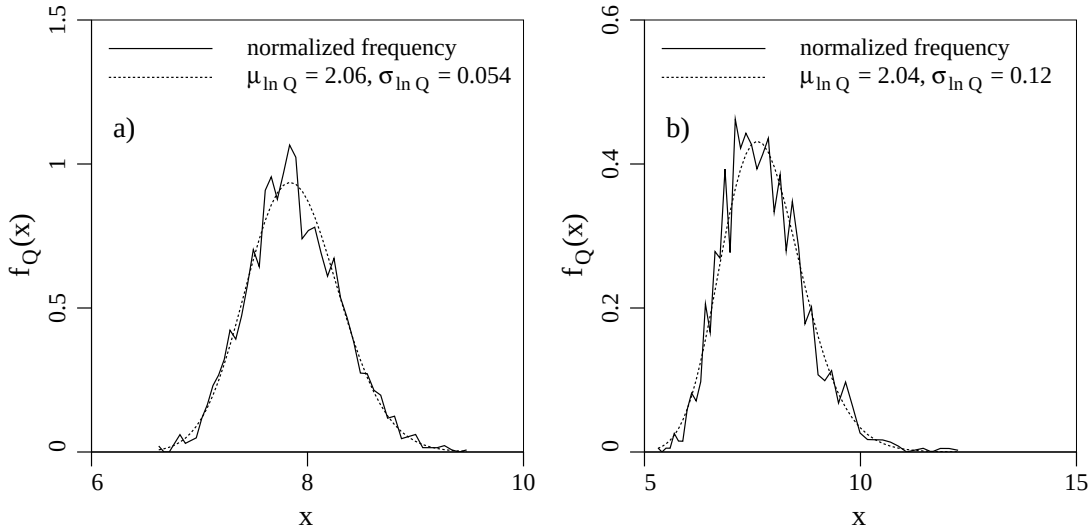

Figure 14. Estimated and fitted lognormal distributions of serviceability limit state loads, Q for a) v = 0.2 and θ = 1 m (p-value = 0.84) and b) v = 0.5 and θ = 1.0 m (p-value = 0.00065).

A pile design involves finding the effective pile perimeter, p, and the pile length, H, required to resist the applied load at an acceptable reliability. If it can be assumed that the pile type is already known, then the problem reduces to finding the required pile length, which involves finding H so that the LRFD equation,

$$\phi_g \hat{R}_u \geq I \sum_i \alpha_i \hat{L}_i \tag{39}$$

is satisfied. Naghibi and Fenton (2009) developed an analytical model which predicts the probability of ultimate limit state failure of a pile,

$$p_f = \mathrm{P}\left[L\frac{\hat{c}}{c} > \frac{I\left[\alpha_L \hat{L}_L + \alpha_D \hat{L}_D\right]}{\phi_g} \right] \tag{40}$$

and this analytical model is compared in Figure 15 to simulation results. The agreement between the two models is excellent.

The analytical failure probability model can be inverted to determine resistance factors required for the ULS design of piles in an LRFD framework. The resistance factors, ϕ_g, required in Eq. 39 to achieve four maximum acceptable failure probability levels (10^{-2}, 10^{-3}, 10^{-4} and 10^{-5}) at moderate level of site understanding (r = 4.5 m) are shown in Figure 16. Again, a worst case correlation length is clearly evident at about the distance between the pile and the sample location.

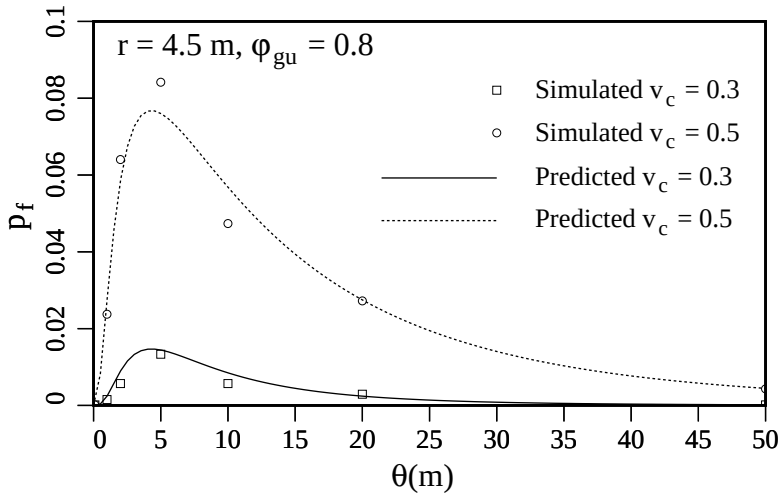

Figure 15. Comparison of analytical and simulation based ultimate limit state pile failure probability.

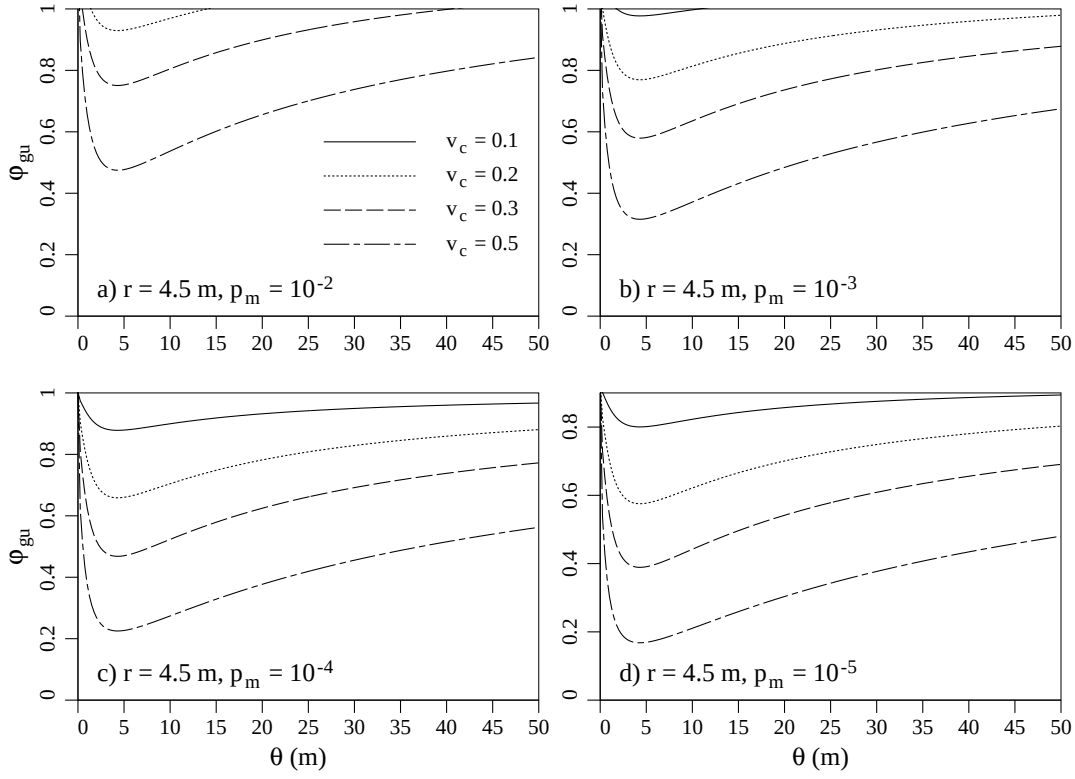

Figure 16. Resistance factors for the ULS design of deep foundations for various maximum acceptable failure probabilities, p_m.

SLOPE STABILITY

Slope stability analysis is a branch of geotechnical engineering that is highly amenable to probabilistic treatment, and has received considerable attention in the literature. The earliest papers appeared in the 1970s (e.g. Matsuo and Kuroda 1974, Alonso 1976, Tang *et al.* 1976, Vanmarcke 1977) and have continued steadily (e.g. D'Andrea and Sangrey 1982, Li and Lumb 1987, Mostyn and Li 1993, Chowdhury and Tang 1987, Whitman 2000, Wolff 1996, Lacasse 1994, Christian *et al.* 1994, Christian 1996, Lacasse and Nadim 1996, Hassan and Wolff 2000, Duncan 2000, Szynakiewicz *et al.* 2002, El-Ramly *et al.* 2002, and Griffiths and Fenton 2004, Griffiths *et al.* 2006 and 2007).

Two main observations can be made in relation to the existing body of work on this subject. First, the vast majority of probabilistic slope stability analyses, while using novel and sometimes quite sophisticated probabilistic methodologies, continue to use classical slope stability analysis techniques (e.g. Bishop 1955) that have changed little in decades, and were never intended for use with highly variable soil shear strength distributions. An obvious deficiency of the traditional slope stability approaches, is that the shape of the failure surface (e.g. circular) is often fixed by the method, thus the failure mechanism is not allowed to "seek out" the most critical path through the soil. Second, while the importance of spatial correlation and local averaging of statistical geotechnical properties has long been recognized by many investigators (e.g. Mostyn and Soo 1992), it is still regularly omitted from many probabilistic slope stability analyses.

In recent years, the authors have been pursuing a more rigorous method of probabilistic geotechnical analysis (e.g. Fenton and Griffiths 1993, Griffiths and Fenton 1993, Paice 1997, Griffiths and Fenton 2000), in which nonlinear finite element methods (Program 6.3 from Smith and Griffiths, 2004) are combined with random field generation techniques. The resulting RFEM is a powerful slope stability analysis tool that does not require *a priori* assumptions relating to the shape or location of the failure mechanism. This section applies the Random Finite Element Method to slope stability risk assessment.

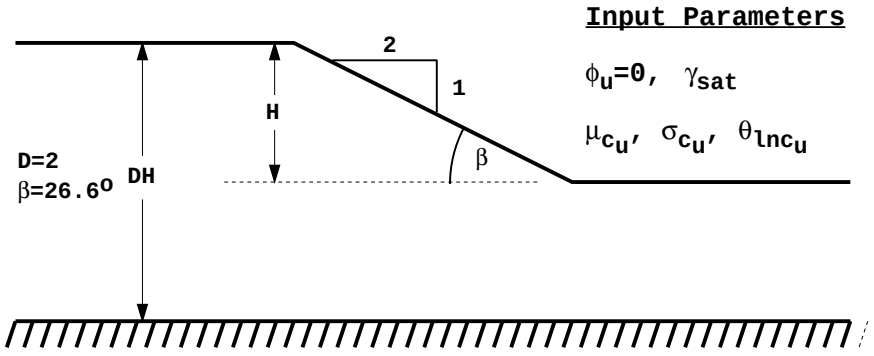

Figure 17. Cohesive slope test problem.

The slope under consideration in this study is shown in Figure 17, and consists of undrained clay, with shear strength parameters ϕ_u = 0 and c_u. In this study, the slope

inclination and dimensions, given by β, H and D, and the saturated unit weight of the soil, γ_{sat} are held constant, while the undrained shear strength c_u is assumed to be a random variable. In the interests of generality, the undrained shear strength will be expressed in dimensionless form c, where $c = c_u/(\gamma_{sat}H)$.

The shear strength c is assumed to be characterized statistically by a lognormal distribution defined by a mean, μ_c, and a standard deviation σ_c. A third parameter, the spatial correlation length $\theta_{\ln c}$ will also be considered here in a non-dimensional form obtained by dividing it by the height of the embankment H,

$$\Theta = \theta_{\ln c}/H \tag{41}$$

In the elasto-plastic RFEM approach, the failure mechanism is free to "seek out" the weakest path through the soil. Figure 18 shows two typical random field realizations and the associated failure mechanisms for slopes with $\Theta = 0.5$ and $\Theta = 2$. The convoluted nature of the failure mechanisms, especially when $\Theta = 0.5$, would defy analysis by conventional slope stability analysis tools. While the mechanism is attracted to the weaker zones within the slope, it will inevitably pass through elements assigned many different strength values. This weakest path determination, and the strength averaging that goes with it, occurs quite naturally in the finite element slope stability method, and represents a very significant improvement over traditional limit equilibrium approaches to probabilistic slope stability, in which local averaging, if included at all, has to be computed over a failure mechanism that is pre-set by the particular analysis method (e.g. a circular failure mechanism when using Bishop's Method).

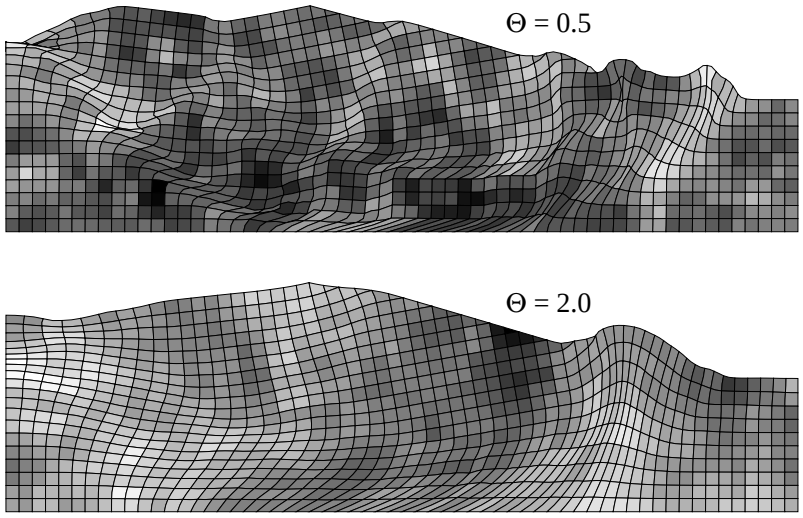

Figure 18. Typical random field realizations and deformed mesh at slope failure for two different spatial correlation lengths. Light zones are weaker.

Fixing the point mean strength at $\mu_c = 0.25$, Figure 19 shows the effect of the coefficient of variation of cohesion, v_c, on the probability of failure for the test problem. Figure 19 also demonstrates that when Θ becomes large, corresponding approximately to a single random variable approach with no local averaging, the probability of failure is

overestimated (conservative) when the coefficient of variation is relatively small and underestimated (unconservative) when the coefficient of variation is relatively high.

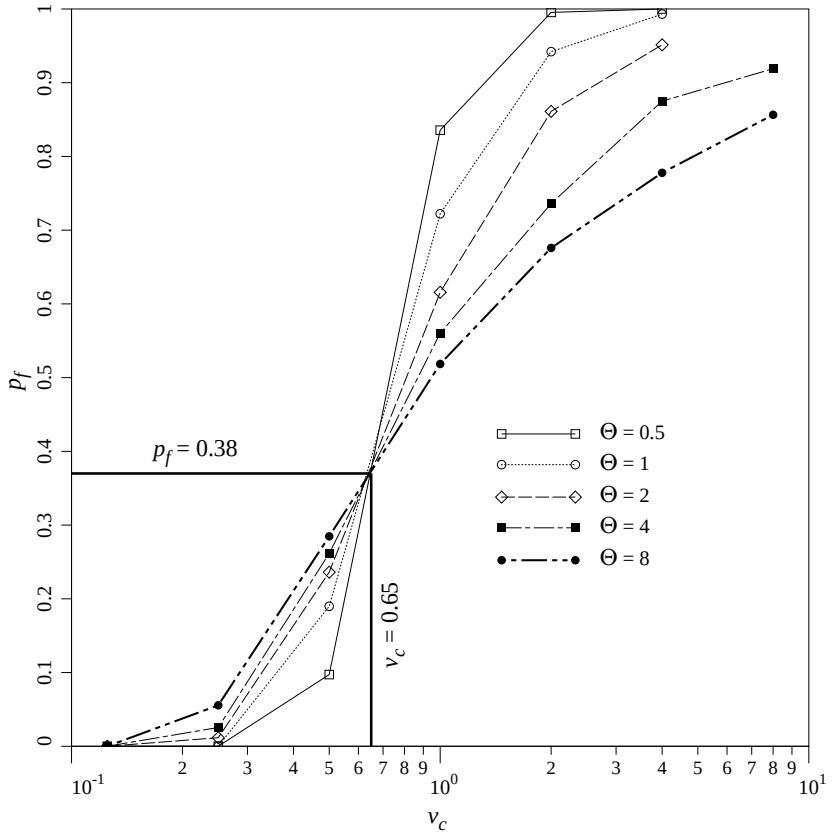

Figure 19. Probability of failure versus coefficient of variation from the random finite element method; the mean is fixed at $\mu_c = 0.25$.

SUMMARY

Uncertainty is a fact of life in all walks of engineering, but particularly so in geotechnical engineering. There is increasing pressure on the geotechnical community to provide risk assessments in conjunction with their designs. This is particularly true in the face of increasing urban and population pressures, climate change uncertainties, and society's decreasing risk tolerance. Thus, while engineering judgement remains essential in any design process, it is becoming increasingly important to make use of probabilistic tools to aid in the decision making process.

The Random Finite Element Method discussed above provides such a tool. Although many other probabilistic methods exist, the integration of random field modeling and the finite element method provides for reduced model error by more realistically modeling the spatial variability of the ground and by allowing failure to occur naturally where it 'wants to'. In addition, the method is easily extended to the study of how site sampling schemes affect as-built reliability, which leads to an improved ability to develop reliability-based geotechnical design codes.

The results presented above cover a variety of common geotechnical problems. Common amongst the results presented is the following observation: In order to reasonably accurately estimate the reliability of a geotechnical system, at least the mean and variance must be known at a site. At most sites, only the mean (and perhaps mean trend) will be known due to limited site investigation budgets. The residual variance (remaining after the mean trend has been determined) is generally obtained by judgement and/or from the literature. In the authors' opinions, the site investigation intensities suggested by codes worldwide are probably sufficient to reduce residual coefficient of variation levels to less than about 30%, excepting, perhaps permeability, so that reasonable resistance factors can be used in the design process.

One of the main problems in determining the reliability of a geotechnical system has to do with how to characterize the spatial variability of the ground. To properly estimate the parameters of spatial variability (e.g. the correlation length) requires very extensive site sampling. Fortunately, it appears that there is usually a 'worst case' spatial variability level which can be used to provide conservative designs. It remains to be seen if the economic losses in the construction of geotechnical systems based on this 'worst case' correlation length are greater or less than the losses due to the increased investigation required to properly estimate the correlation length. Much work is required to decide upon this issue. However, it appears to the authors that the reliability levels based on the worst case correlation length agree with those adopted by most modern geotechnical design codes, and so at this point, adopting these conservative estimates appears reasonable.

Finally, the results presented above are still very generic, in that they describe the 'average site'. Their value is in providing the geotechnical community with knowledge about the basic probabilistic behaviour of geotechnical systems – in particular how spatial variability affects failure probability. In the future, we need to focus on site specific behaviour: Individual sites will generally not have isotropic correlation structures, will often be layered, and may not be well represented by a single spatially variable random field. While the methodology presented above is reasonably easily extended in concept to the modeling of a specific site, the computer models to do so have not yet been fully developed for all problems. Such advancements are in need of further work, but are coming.

REFERENCES

AASHTO (2007). *LRFD Bridge Design Specifications*, American Association of State Highway and Transportation Officials, Washington, DC.

Allen, D.E. (1975). "Limit States Design – A probabilistic study," *Can. J. Civ. Engrg.*, **36**(2), 36–49.

Alonso, E.E. (1976). "Risk analysis of slopes and its application to slopes in Canadian sensitive clays," *Géotechnique*, **26**, 453–472.

Australian Standard (1995). *Piling – Design and Installation*, AS 2159–1995, Sydney, Australia.

Australian Standard (2004). *Bridge Design, Part 3: Foundations and Soil-Supporting Structures*, AS 5100.3–2004, Sydney, Australia.

Australian Standard (2002). *Earth-Retaining Structures*, AS 4678–2002, Sydney, Australia.

Becker, D.E. (1996). "Eighteenth Canadian Geotechnical Colloquium: Limit states design for foundations. Part II. Development for the National Building Code of Canada," *Can. Geotech. J.*, **33**, 984–1007.

Bishop, A.W. (1955). "The use of the slip circle in the stability analysis of slopes," *Géotechnique*, **5**(1), 7–17.

Canadian Geotechnical Society (1992). *Canadian Foundation Engineering Manual*, 3rd Ed., Montreal, Quebec.

Canadian Geotechnical Society (2006). *Canadian Foundation Engineering Manual*, 4th Ed., Montreal, Quebec.

Casagrande, A. (1937). "Seepage through dams," *Journal of the New England Water Works Association*, **51**(2), 131–172.

Cedergren, H.R. (1967). *Seepage, Drainage and Flow Nets*, John Wiley & Sons, Chichester, New York.

Cherubini, C. (2000). "Reliability evaluation of shallow foundation bearing capacity on c', ϕ' soils," *Can. Geotech. J.*, **37**, 264–269.

Chowdhury, R.N. and Tang, W.H. (1987). "Comparison of risk models for slopes," *Proc. 5th Int. Conf. on Applications of Statistics and Probability in Soil and Structural Engineering*, Vol. 2, 863–869.

Christian, J. T., Ladd, C. C. and Baecher, G. B. (1994). "Reliability applied to slope stability analysis," *ASCE J. Geotech. Engrg.*, **120**(12), 2180–2207.

Christian, J.T. and Carrier, W.D. (1978). "Janbu, Bjerrum and Kjaernsli's chart reinterpreted," *Can. Geotech. J.*, **15**, 123–128.

Christian, J.T. (1996). "Reliability methods for stability of existing slopes," *Uncertainty in the geologic environment: From theory to practice*, al, C.D., ed., ASCE, Geotechnical Special Publication No. 58, New York, 409–418.

D'Andrea, R.A. and Sangrey, D.A. (1982). "Safety Factors for Probabilistic Slope Design," *ASCE J. Geotech. Engrg.*, **108**(GT9), 1101-1118.

Das, B.M. (2000). *Fundamentals of Geotechnical Engineering*, Brooks/Cole, Pacific Grove, California.

Duncan, J.M. (2000). "Factors of safety and reliability in geotechnical engineering," *ASCE J. Geotech. Geoenv. Engrg.*, **126**(4), 307–316.

EN 1997-1 (2003). *Eurocode 7 Geotechnical design – Part 1: General rules*, CEN (European Committee for Standardization), Brussels.

El-Ramly, H., Morgenstern, N.R. and Cruden, D.M. (2002). "Probabilistic slope stability analysis for practice," *Can. Geotech. J.*, **39**, 665–683.

Engineers, Institution of Civil (1991). *Inadequate Site Investigation*, Thomas Telford, London.

Fenton, G. A., Zhang, X.Y. and Griffiths, D.V. (2007). "Reliability of shallow foundations designed against bearing failure using LRFD," *Georisk*, **1**(4), 202–215.

Fenton, G. A., Zhang, X.Y. and Griffiths, D.V. (2008). "Load and resistance factor design of shallow foundations against bearing failure," *Can. Geotech. J.*, **45**(11), 1556-1571.

Fenton, G.A. (1994). "Error evaluation of three random field generators," *ASCE J. Engrg. Mech.*, **120**(12), 2478–2497.

Fenton, G.A. and Vanmarcke, E.H. (1990). "Simulation of random fields via Local Average Subdivision," *ASCE J. Engrg. Mech.*, **116**(8), 1733–1749.

Fenton, G.A. and Griffiths, D.V. (1993). "Statistics of block conductivity through a simple bounded stochastic medium," *Water Resources Res.*, **29**(6), 1825–1830.

Fenton, G.A. and Griffiths, D.V. (2003). "Bearing capacity prediction of spatially random $c - \phi$ soils," *Can. Geotech. J.*, **40**(1), 54–65.

Fenton, G.A. and Griffiths, D.V. (2008). *Risk Assessment in Geotechnical Engineering*, John Wiley & Sons, New York.

Fenton, G.A., Griffiths, D.V. and Cavers, W. (2005). "Resistance factors for settlement design," *Can. Geotech. J.*, **42**(5), 1422–1436.

Griffiths, D.V. and Fenton, G.A. (2000). "Influence of soil strength spatial variability on the stability of an undrained clay slope by finite elements," *Slope Stability 2000*, ASCE Geotechnical Special Publication No. 101, New York, 184–193.

Griffiths, D.V. and Fenton, G.A. (1993). "Seepage beneath water retaining structures founded on spatially random soil," *Géotechnique*, **43**(4), 577–587.

Griffiths, D.V., Fenton, G.A. and Denavit, M.D. (2007). "Traditional and advanced probabilistic slope stability analysis," *Probabilistic Applications in Geotechnical Engineering, GSP No. 170, ASCE*, Proc. Geo-Denver 2007 Symposium, Denver, Colorado, .

Griffiths, D.V., Fenton, G.A. and Ziemann, H.R. (2006). "The influence of strength variability in the analysis of slope failure risk," *Geomechanics II, Proc. 2nd Japan-US Workshop on Testing, Modeling and Simulation, ASCE*, Lade, P.V. and Nakai, T., eds., GSP No. 156, Kyoto, Japan, 113–123.

Griffiths, D.V. and Fenton, G.A. (1995). "Observations on two- and three-dimensional seepage through a spatially random soil," *Proceedings of the Seventh International Conference on Applications of Statistics and Probability in Civil Engineering*, Paris, France, 65–70.

Griffiths, D.V. (1984). "Rationalised charts for the method of fragments applied to confined seepage," *Géotechnique*, **34**(2), 229–238.

Griffiths, D.V. and Fenton, G.A. (2004). "Probabilistic slope stability analysis by finite elements," *ASCE J. Geotech. Geoenv. Engrg.*, **130**(5), 507–518.

Harr, M.E. (1962). *Groundwater and Seepage*, McGraw-Hill, New York.

Hassan, A.M. and Wolff, T.F. (2000). "Effect of deterministic and probabilistic models on slope reliability index," *Slope Stability 2000, Geotechnical Special Publication No. 101*, ASCE, New York, 194–208.

Jaksa, M.B., Goldsworthy, J.S., Fenton, G.A., Kaggwa, W.S., Griffiths, D.V., Kuo, Y.L. and Poulos, H.G. (2005). "Towards reliable and effective site investigations," *Géotechnique*, **55**(2), 109–121.

Janbu, N., Bjerrum, L. and Kjaernsli, B. (1956). "Veiledning ved losning av fundamenteringsoppgaver," *Norwegian Geotechnical Institute Publication 16*, Oslo, 30–32.

Lacasse, S. (1994). "Reliability and probabilistic methods," *Proc. 13th Int. Conf. on Soil Mechanics Foundation Engineering*, 225–227.

Lacasse, S. and Nadim, F. (1996). "Uncertainties in characterising soil properties," *ASCE Uncertainties'96 Conference Proceedings*, Benson, C.H., ed., Madison, Wisconsin, USA, 49–75.

Law, A.M. and Kelton, W.D. (2000). *Simulation Modeling and Analysis*, (3rd Ed.), McGraw-Hill, New York, NY.

Lewis, P.A.W. and Orav, E.J. (1989). *Simulation Methodology for Statisticians, Operations Analysts, and Engineers*, Vol. 1, Wadsworth & Brooks, Pacific Grove, California.

Li, K.S. and Lumb, P. (1987). "Probabilistic design of slopes," *Can. Geotech. J.*, **24**, 520–531.

Matsuo, M. and Kuroda, K. (1974). "Probabilistic approach to the design of embankments," *Soils and Foundations*, **14**(1), 1–17.

Meyerhof, G. G. (1951). "The ultimate bearing capacity of foundations," *Géotechnique*, **2**(4), 301–332.

Meyerhof, G. G. (1963). "Some recent research on the bearing capacity of foundations," *Can. Geotech. J.*, **1**(1), 16–26.

Meyerhof, G.G. (1970). "Safety factors in soil mechanics," *Can. Geotech. J.*, **7**, 349–355.

Meyerhof, G.G. (1982). "Limit States Design in Geotechnical Engineering," *Structural Safety Journal*, **1**, 67–71.

Mostyn, G.R. and Soo, S. (1992). "The effect of autocorrelation on the probability of failure of slopes," *Proc. 6th Australia, New Zealand Conf. on Geomechanics: Geotechnical Risk*, 542–546.

Mostyn, G.R. and Li, K.S. (1993). "Probabilistic slope stability – State of play," *Proc. Conf. on Probabilistic Methods in Geotechnical Engineering, Balkema*, Li, K.S. and Lo, S.-C. R., eds., Rotterdam, The Netherlands, 89–110.

Naghibi, M. and Fenton, G.A. (2009). "Resistance factors for the ultimatelimit state design of deep foundations in undrained soils," *Can. Geotech. J.*, under review.

National Research Council (2005). *National Building Code of Canada*, National Research Council of Canada, Ottawa.

National Research Council (2006). *User's Guide – NBC 2005 Structural Commentaries (Part 4 of Division B)*, 2nd Ed., National Research Council of Canada, Ottawa.

Paice, G.M. (1997). "Finite element analysis of stochastic soils," Ph.D. Thesis, University of Manchester , Civil Engineering, Manchester, U.K..

Pavlovsky, N.N. (1933). "Motion of water under dams," *Proceedings of the 1st Congress on Large Dams*, Stockholm, 179–192.

Phoon, K-K. and Kulhawy, F.H. (1999). "Characterization of geotechnical variability," *Can. Geotech. J.*, **36**, 612–624.

Prandtl, L. (1921). "Uber die Eindringungsfestigkeit (Harte) plastischer Baustoffe und die Festigkeit von Schneiden," *Zeitschrift fur angewandte Mathematik und Mechanik*, **1**(1), 15–20.

Smith, I.M. and Griffiths, D.V. (1982). *Programming the Finite Element Method*, (2nd Ed.), John Wiley & Sons, New York, NY.

Smith, I.M. and Griffiths, D.V. (2004). *Programming the Finite Element Method*, (4th Ed.), John Wiley & Sons, New York, NY.

Sokolovski, V.V. (1965). *Statics of Granular Media*, 270 pages, Pergamon Press, London, UK.

Szynakiewicz, T., Griffiths, D.V. and Fenton, G.A. (2002). "A probabilistic investigation of c', ϕ' slope stability," *Proceedings of the 6th International Congress on Numerical Methods in Engineering and Scientific Applications, CIMENICS'02, Pub. Sociedad Venezolana de Métodos Numéricos en Ingeniería*, CI 25–36.

Tang, W.H., Yuceman, M.S. and Ang, A.H.S. (1976). "Probability-based short-term design of slopes," *Can. Geotech. J.*, **13**, 201–215.

Terzaghi, K. (1943). *Theoretical Soil Mechanics*, John Wiley & Sons, New York, NY.

Vanmarcke, E.H. (1977). "Probabilistic Modeling of Soil Profiles," *ASCE J. Geotech. Engrg.*, **103**(GT11), 1227–1246.

Vanmarcke, E.H. (1984). *Random Fields: Analysis and Synthesis*, The MIT Press, Cambridge, Massachusetts.

Verruijt, A. (1970). *Theory of Groundwater Flow*, MacMillan & Co. Ltd., London.

Vesic, A.S. (1977). *Design of Pile Foundations*, in *National Cooperative Highway Research Program Synthesis of Practice No. 42*, Transportation Research Board, Washington, D.C..

Vick, S.G. (2002). *Degrees of Belief: Subjective Probability and Engineering Judgement*, American Society of Civil Engineers, Reston, Virginia.

Vijayvergiya, V.N. and Focht, J.A. (1972). "A new way to predict capacity of piles in clay," *Fourth Offshore Technology Conference*, Houston, Paper 1718.

Whitman, R.V. (2000). "Organizing and evaluating uncertainty in geotechnical engineering," *ASCE J. Geotech. Geoenv. Engrg.*, **126**(7), 583–593.

Wolff, T.F. (1996). "Probabilistic slope stability in theory and practice," *Uncertainty in the Geologic Environment: From Theory to Practice, Geotechnical Special Publication No. 58*, al., C.D. Shackelford et al., ed., ASCE, New York, 419–433.

Wolff, T.H. (1985). "Analysis and design of embankment dam slopes: a probabilistic approach," Ph.D. Thesis, Purdue University, Lafayette, Indiana.